Study of the momentum, angular resolutions of the mesons and missing mass resolution of the $p(K^-, K^+)\Xi^-$ reaction using the KURAMA magnet in the E07 experiment

Iskendir Abzal

Master's Thesis
Department of Physics, Graduate School of Science
OSAKA UNIVERSITY

31 July 2017

Abstract

Investigation of the nuclei with the strangeness and hyperon-nucleon interaction is one of the achievements of nuclear physics. The purpose of the E07 experiment, at J-PARC (Japan Proton Accelerator Research Complex) K1.8 beam-line, is a systematic study of double strangeness (S = -2) systems via nuclear emulsion. The (K^-, K^+) charge exchange reaction, $p(K^-, K^+)\Xi^-$, is detected using KURAMA spectrometer setup. Thereafter, Ξ^- hyperons produced and react with protons in the nucleus and double Λ hypernuclei are formed by generating two Λ particles. In this experiment, scattering K^+ particles are measured with the KURAMA spectrometer sets.

The aim of this research is to explore the performance of the KURAMA spectrometer by studying the effect of the position resolutions of tracking detectors and multiple scattering by materials. All analysis are made up step by step.

Momentum resolution. We estimate both K^- and π^- mesons by selection cuts from trigger information. For the estimation of the resolution of momentum, 4 different momenta were used from beamthrough: 1.8,1.4,1.2 and 1.0 GeV/c. The momentum resolution of scattered K^- is analysed by using KURAMA spectrometer with magnetic field strength of 0.72T.

Angular resolution. Angle defined by drift chambers (SDC1,2,3) which is placed before and after KURAMA magnet. Also small-scattering angle before and after target position are estimated from beamthrough analysis. After analysing the data, angular resolution (K^-,π^-) is calculated by hand by considering E07 experiment geometry.

Missing mass resolution. The momentum of scattered K^+ particles are measured with the KURAMA spectrometer and the missing mass spectrum of Ξ^- is identified from polyethylene CH_2 run. After beam-through analysis, the result of momentum and angular resolutions are applied to obtain the expected missing mass resolution. Expected missing mass resolution is less than $\sim 17 MeV/c^2$ at the 1.8 GeV/c beam.

Finally, the comparison of expected and analysis result will be made for the momentum, angular and missing mass analysis.

Contents

List of Figures

List of Tables

Chapter 1

Introduction

1.1 Introduction

Nowadays, the investigation of the nuclei with strangeness and hyperon-nucleon interaction is one of achievements of nuclear physics. By definition, a hyper nuclei is a nucleus that are associated with hyperons (Σ, Ξ, Λ). The Baryon-Baryon (BB) interactions and the Baryon's property in the nuclear substance can be explained properly by studying of hypernuclei. There has been an assumption that, nucleons actually move freely inside the nucleus due to large distance between nucleons comparing to the radius of nucleon core.

1.1.1 Study of hyperons

Baryons, which contain **s** – quarks are collectively referred to call as hyperons. The neutron and the proton, together the nucleons, are the well known baryons. Hyperons , the Λ, Σ, Ξ and Ω, are differentiated between them by their isospin and the sum of the s – quarks that they hold within the structure.The anti hyperons possess the positive strangeness +1, +2, +3, respectively. Table 1.1 represents the classification of hyperons in the ground state with quark composition, the mass, isospin, spin and the life time. In the experiment,usually the baryons (hyperons) are produced in the *production experiment* by bombarding experimental target with beam of protons,pions or kaons with high energy.

1.1.2 E07 experiment. Double hypernuclei search experiment

Experimental study of double-Λ and Ξ hypernuclei is a unique evidence to understand the Ξ- interaction and Λ-Λ interaction,however the investigation of those type of hypernucleis is very difficult. The purpose of E07 experiment is to investigate the double strangeness world with emulsion method. Historically believed that the nuclear emulsion is an appropriate detector for the investigation of the hyperon systems. The information of regarding

Table 1.1: The classification of the hyperons in the ground state.

	Quark composition	Mass[MeV/c^2]	Isospin	Spin	Life[s]
Λ^0	uds	1115.6	0	1/2	2.60×10^{-10}
Σ^+	uus	1189.4	1	1/2	0.8×10^{-10}
Σ^0	uds	1192.5	1	1/2	7.4×10^{-20}
Σ^-	dds	1197.4	1	1/2	1.47×10^{-10}
Ξ^0	uss	1314.9	1/2	1/2	2.9×10^{-10}
Ξ^-	dss	1321.3	1/2	1/2	1.63×10^{-10}
Ω^-	sss	1672.5	0	3/2	8.21×10^{-11}

to double starngenes nucleus in the emulsion has been investigated more than thirty years ago [7][8].

Over 50 years ago, Danysz et al., showed the information of four hyperfragments of the Ξ^- hyperon events which stopped in nuclear emulsion system. The next generation of emulsion experiment, the E176, was performed in 1991. In the experiment, the quasi-free 'p'$(K^-, K^+)\Xi^-$ reaction is investigated by tagging the events into emulsion system at KEK. In the E176, there was a confirmation of the existence of the double-Λ hypernucleus as a result of around 80 Ξ^- hyperon stops [7].

In 1998, the E373 experiment was performed and the experimental method was almost similar to E176 to investigate the energy of double-Λ interaction through the detecting the Λ-hypernuclei. The diamond target was settled up to probe the Ξ-hyperon. In the emulsion-counter, the tracks of the Ξ- hyperon can be known from their traces in the emilsion system.

1.1.3 Ξ^- hyperon and ΞN interaction

The purpose of the E07 experiment is study of double strangeness nuclei with the hybrid-emulsion method. As a purpose of that, Ξ^- hyperon will be investigated to understand the baryon's world with $S = -2$ nuclei. Historically, there were existence of double strangeness nuclei Ξ^- with the emulsion method over 30 years ago. Study of Ξ^- hyperon is important to understand the properties of double strangeness system. One of the crucial parameters of studying double strangeness nuclei is the measurement of its mass (binding energy). In the E373 experiment, the earliest experiment before the E07, several hundreds of Ξ^- traces were obtained by emulsion system. As a result of emulsion analysis, among Ξ^- stops 2 single Λ hypernuclei and 6 double hypernucleus events had been detected owing to decay topology of them. Therefore in the E07, stopping Ξ^- events are expected to be higher 10 times than that of the E373 experiment analysis.

ΞN interaction will be studied by probing the X-rays from the Ξ^- events. The energy measurement of X-ray of the double strangeness system is going perform for the first time in the E07 experiment. The emulsion comprised up as a combination of C, N, O, Ag *and* Br elements. Ge detectors examine X-rays from Ξ^- capture at the emulsion. In accordance with the X-ray of the following $\Xi^- - Ag$ and $\Xi^- - Br$ atoms, the $\Xi^- N$ interaction will be investigated.

One can see the classification table for baryons in figure 1.1 [4].

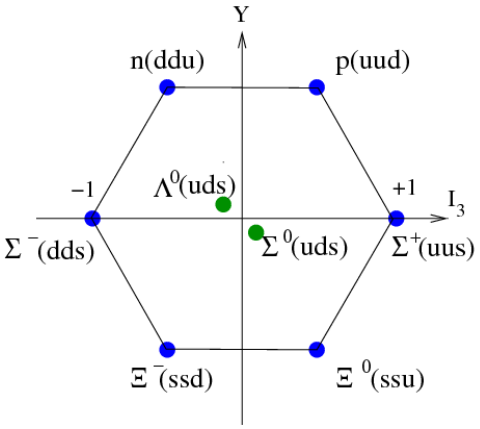

Figure 1.1: The classification of baryon octet for spin 1/2. I_3 and Y *depict z component of isospin and hyper charge.*

Spectrum of the baryon's mass is drafted in figure 1.2 as a function of strangeness and isospin.

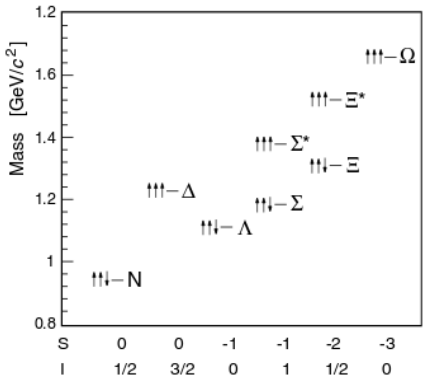

Figure 1.2: The decuplet and octet baryons mass [1].

1.1.4 The purpose of this reserch

This research is based on the E07 experiment, the goal of the this research is to investigate the performance of the KURAMA spectrometer by studying the effect of the position resolutions and multiple scattering by materials. Moreover,the sets of resolutions, the momentum, angle and missing mass resolution, can be checked out for our comparison with data analysis.The investigation of the momentum, the angle resolutions is performed by beamthrough run. In this study we used beamthrough run with 1.8,1.4,1.2 and 1.0 GeV/c momentum. The taken results are applied to estimate expected missing mass from $p(K^-, K^+)\Xi^-$ reaction. The polyethylene (CH_2) run is used to probe the missing mass resolution of Ξ^-hyperon. Not only analysis could be done but also rough estimation of missing mass has been provided by comparing with the experimental data. The important point of the missing masses spectrum is belongs to the following reaction: $K^- + target- > K^+ + \Xi^-$. Where $p(proton)$ is served as a target from polyethylene structure.

$$\Delta M^2 = (\frac{\delta M}{\delta p_{K-}})^2 \delta p_{K-}^2 + (\frac{\delta M}{\delta p_{K+}})^2 \delta p_{K+}^2 + (\frac{\delta M}{\delta \theta})^2 \delta \theta^2 \tag{1.1}$$

The mathematical expression (1.1) of missing mass resolution tells that the momentum and angular resolution contributions are important to obtain good resolution of expected missing mass.
Generally, the mass of a particles are crucial physics parameters to identify them. However, it is impossible to measure directly the particle's mass. That's why the equation (3.5 in chapter 3) allows us to determine the missing mass of the particle in the (K^-, K^+)reaction.

Chapter 2

Experimental Setup

2.1 Experimental facility. J-PARC and K1.8 Beamline

2.1.1 Overview. General information of J-PARC

J-PARC (Japan Proton Accelerator Research Center) is engaged in investigating deeply the following diverse branches of science field, namely, nuclear physics,particle physics, material science, the technology of nuclear field and life science, by using high intensity proton accelerator facilities. Moreover, this research complex often provides the highest beam power in the world.
Mainly, J-PARC is composed of four facilities, they are – The Hadron Experimental facility, the Neutron Facility, The Material Science including Life facility and The Accelerator-Driven Transmutation system experimental facility amenably demonstrated in Figure 2.1.

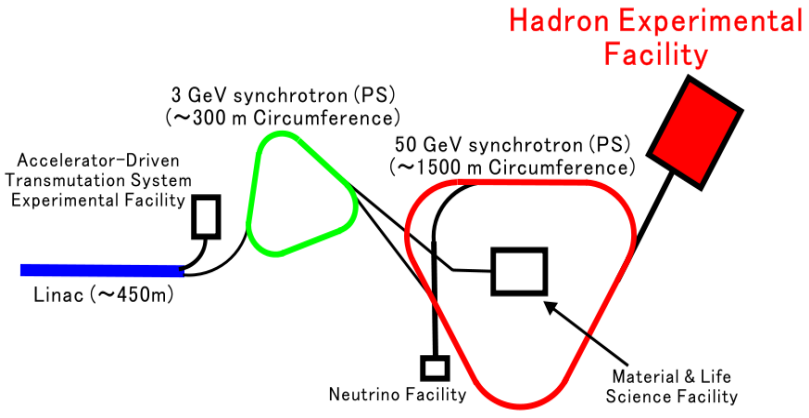

Figure 2.1: Schematic drawing of J-PARC.

Commonly, a subatomic particle experiment, particle physics experiment and strangeness nuclear experiment will be carried out in a hadron experimental building.
In the first instance, hydrogen is elaborated from the ion source and accelerated by LINAC system to around 400 MeV(50 mA). Then accelerated hydrogen is transformed to a proton, converted proton towards to Rapid-Cycling Synchrotron (RCS) for speeding – up its energy value from 400 MeV till 3 GeV (333 A).
Eventually, the proton is accelerated by Main Ring (MR) up to 30 GeV (15 A). After all the acceleration procedures the 30 GeV proton beams are ensured to the hadron facility and the secondary hadron beam is extracted from them and used for experiment.

2.1.2 Hadron experimental facility

A systematic study of double strangenes (S=-2) experiment, namely E07 experiment, were performed in the hadronic experimental facility. The Hadron hall is comprised from several fundamental parts,namely they are: a primary beam line, an assorted secondary beam lines and the main installiation parts(equipmenmts) for the holding experiments,in Figure 2.2. An exaggerated proton beam is transferred from the Main Ring to the hadron experimental building to fabricate the secondary beams that used for our experiment.

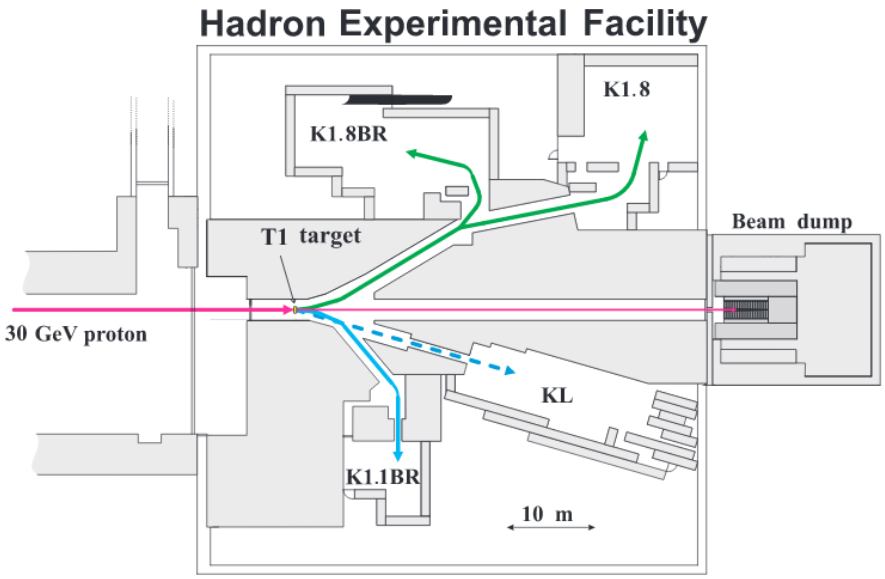

Figure 2.2: A schematic view of Hadron Experimental Facility.The proton beam taken out from the MR is used to extract the secondary particle generation by irradiating T1 target, and the secondary beam is transported to K1.8, K1.8 BR, KL beamlines.

After hitting off the production target, which named T1 target, at the production

target many types of the secondary beams (kaons, pions and so forth) will be available concurrently for holding experiment. As mentioned before, at the first target subordinates beam lines such as Kaons,Pions delivered simultaneously to Hadron Hall and they are optimized in the K1.8 beam line by obtaining the diverse momenta value, 1.8,1.4,1.2 and 1.0 GeV/c respectively.

2.1.3 K1.8 beam line

There are two electric separators (ES1 and ES2) in the K1.8 beam line which are located in the way the incoming beam and their primary function is to separate kaons from pions in the unseparated beam. The expected beam momentum is 1.8 GeV/c (K^-) at the E07 experiment. An expected high purity kaon (K^-) beam is around $3 * 10^5$ for the one spill. The ratio of K^-/π^- is designed to be 6 at the 4.8 second in the cycle (spill time 2.0 sec). The complete length of the K1.8 beam line is $\sim 46m$. The K1.8 beam line schema is represented in figure 2.3 and Table 2.1 show the specifications of K1.8 beam-line.

Table 2.1: The specifications of the K1.8 beamline

Momentum resolution	$3.3 \times 10^{-4} FWHM$
Maximum momentum	2.0 GeV/c
Bending angle	64°

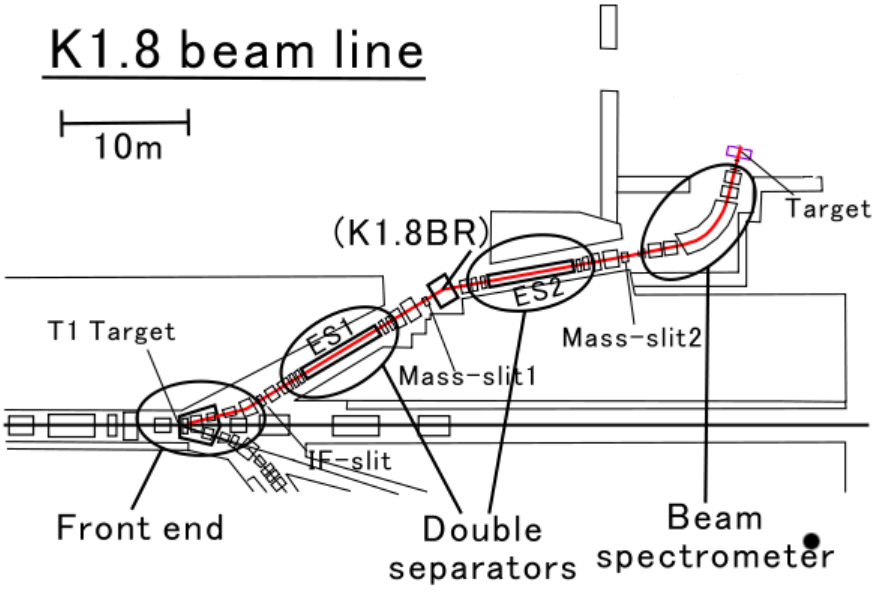

Figure 2.3: A sketch of K1.8 beamline

2.1.4 The E07 experiment setup

By proposal, an emulsion method are used to investigate double strangeness system by detecting Ξ^--hyperons by using the emulsion-hybrid method. Via emulsion system, we can access to the information of short tracks of hyperfragments and the decay vertices of Ξ^- hyperon. The main product of emulsion-hybrid method is *the emulsion plates*. According to track lengths in emulsion, the nuclei are sorted out in two types, light (C,N,O) and heavy (Br,Ag) elements. In figure 2.4 the E07 setup is given.

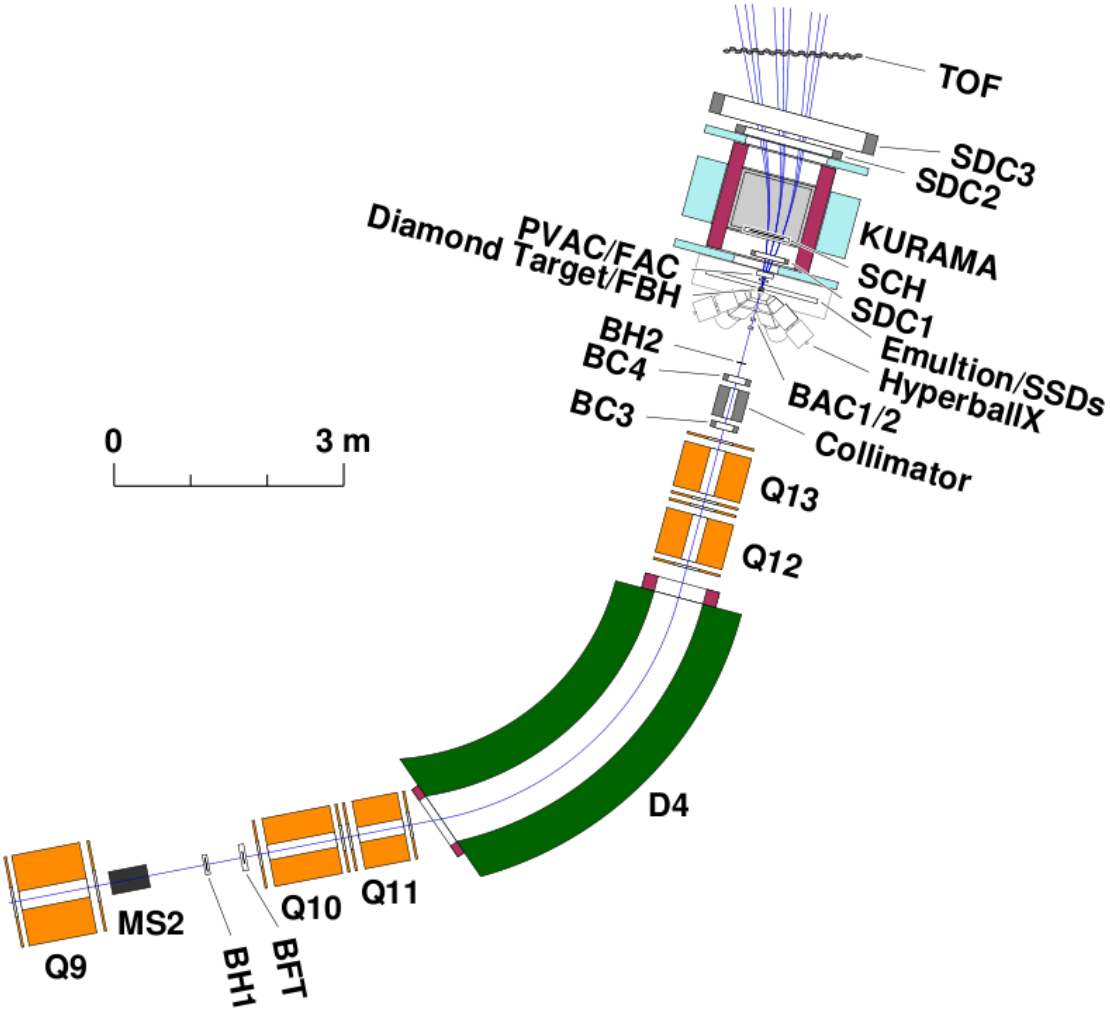

Figure 2.4: Schematic view of the E07 experiment

2.2 K1.8 beam-line spectrometer

Usually, we call *K1.8 beam-line spectrometer* between MS2 to target including BH2. Figure 2.5 shows the K1.8 beam-line spectrometer's schematic view. The incident beam is analysed with the K1.8 beam-line spectrometer. The set of magnets in the E07 experiment, namely $Q10$, $Q11$, $D4$, $Q12$ and $Q13$, are used as the K1.8 beam-line spectrometer. Incident beam is focused to experimental target by $Q12$ and $Q13$ quadruple magnets. Basically, K1.8 beam-line spectrometer serves not only focusing beam, but also a momentum of beam is measured as well. The incident K^- is analysed event by event in the K1.8 beam-line spectrometer.

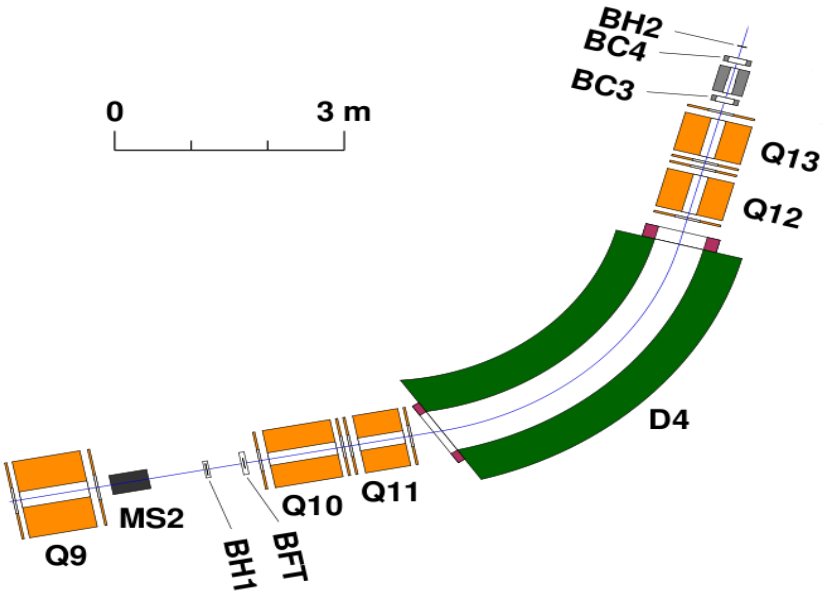

Figure 2.5: K.18 beam-line spectrometer.

2.3 KURAMA spectrometer

The arrangement of the KURAMA spectrometer setup is substantially similar to the E373 experiment. The momentum of the outgoing particles (K^+ or π^+) is measured using the KURAMA magnet and Multiwire Drift Chambers (MWDC). The main function of using the KURAMA magnet is because of having a large acceptance for the outgoing K^+, in a place of SKS (Superconducting Kaon Spectrometer) magnet at the K1.8 beam line. The KURAMA dipole magnet is used to achieve more and more detection efficiency of K^+ outgoing mesons. The scattered particles can be detected by the KURAMA spectrometer which seen in figure 2.6.

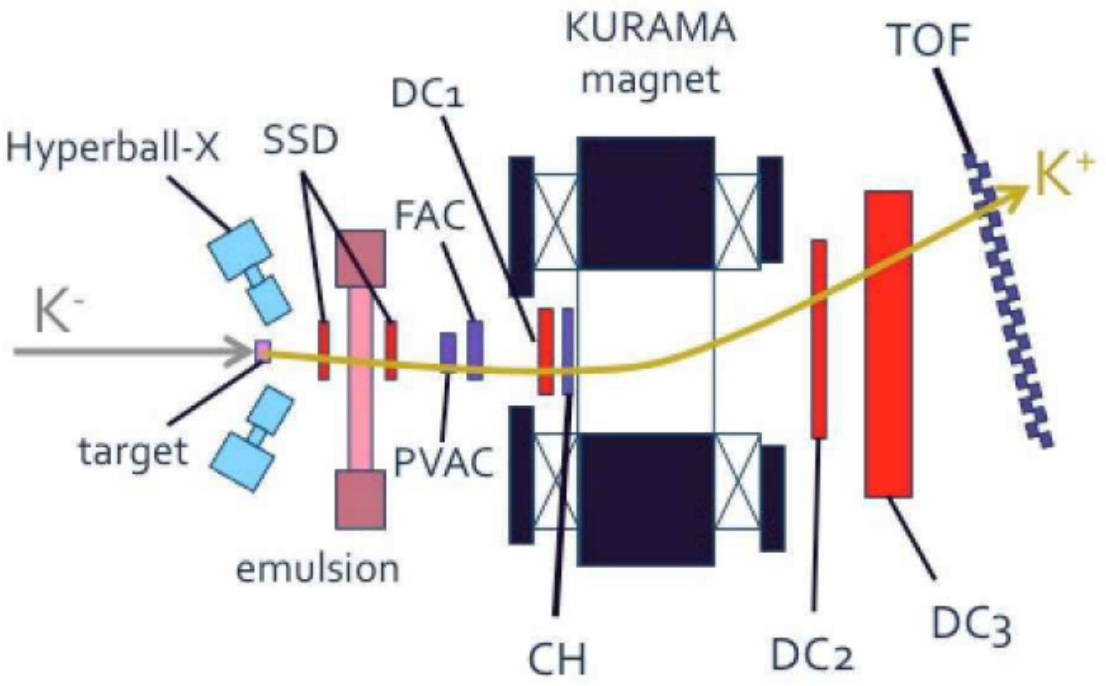

Figure 2.6: KURAMA spectrometer setup

2.3.1 Time Counters

There were two time counters (BH1 and BH2) for measuring the time-of-flight of incoming group of particles such as π^- and K^-. In the offline analysis by the help of timing counters the K^- particles were selected as an incident particle. The Beam Hodoscope (BH1) is located upstream of $QQD4QQ$ magnets system and the BH2 was supplied upstream of the target. The BH1 is a plastic scintillation detector that consists of eleven segments, and signals can be read by both upright ends, the upper and lower PhotoMultiplier Tubes (PMT), HPK H6524 MOD.The figure 2.7 represents the structure of BH1.

BH2 is a plastic scintillation detector which made up by single segment structure having a size of $120mm \times 40mm \times 6mm$. The signals of detector revealed by both,up- and down-right photomultiplier tubes H10570. Also, BH2 serves as a start timing of DAQ system. The distance between the BH1 and BH2 was around 10.334 m.

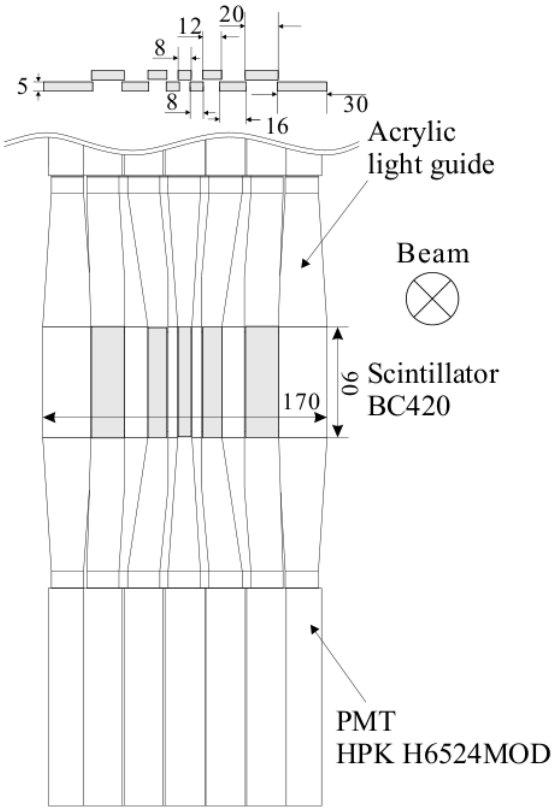

Figure 2.7: The structure of BH1.[11]

2.3.2 KURAMA magnet

The KURAMA magnet was excited up to 0.72 T in the present experiment. The KURAMA dipole magnet has a large acceptance, and the extent of the gap pole is 50 cm high, 100 cm wide and the length is 80 cm. In this experiment, the magnet was controlled to obtain the magnetic strength - 0.72 Tesla with the central magnetic field. The magnet is placed 150 mm horizontally from the beam axis and 1.74 m from the experimental target having an acceptance of 200 msr. The performances of several spectrometers are demonstrated in Table 2.2[9].

Table 2.2: The performances of several spectrometers at KEK.

Name	Acceptance [msr]	Maximum momentum [GeV/c]
SKS	100	1.7
KURAMA	200	2.0
48D48	20	1.0

2.3.3 Drift chambers

In the KURAMA spectrometer, to obbtain the trajectory of scattered particles three sets of the Multiwire Drift Chambers were used. At the entrance of KURAMA magnet, a multiwire drift chamber (SDC1) is located. The next two drift chambers SDC 2-3 were installed between the KURAMA and TOF wall. The wire spacing of drift chambers were 6, 9 and 20 mm having a honeycomb structure in shape.

Table 2.3: The list of specifications of drift chambers in the KURAMA spectrometer.

Name	Active area,W×H(mm)	wire space (mm)	Wires	layers
SDC1	400×252	6	$vv\prime xx\prime uu\prime$	6
SDC2	1186.5×1186.5	9	xx$\prime yy\prime$	4
SDC3	1920×1280	20	yy$\prime xx\prime$	4

2.3.4 Charge Hodoscope

The charge hodoscope (CH) is comprised from 64 segments and its an effective area is 674 mm (high) · 450 mm (wide). The CH were installed upstream of the pole of the KURAMA magnet. The size of CH is: $2mm \times 11.5mm$ [thickness*width] and can be read by MPPC (multi-pixel photon counters).

2.3.5 Aerogel counters

PVAC and FAC

The KURAMA spectrometer setup is included two types of aerogel counters, such as PVAC and FAC. The former type aerogel counter is utilised as a proton veto counter. PVAC hgelps to eradicate the scattered proton. The latter counter, FAC (Forward aerogel counter) helps to eliminate the scattered π^+. An effective area is $117mm \times 117mm$ for PVAC, while FAC has $220mm \times 180mm$. The refractive index were 1.12 and 1.05 for PVAC (thickness 30mm) and FAC(thickness 60mm), respectively. Calculation of the thickness of aerogel counters due to

$$n = 1 + 0.21 \cdot \rho \tag{2.1}$$

Therefore, the thickness of proton and pion veto counters are 1.7143 and $1.4286 g/cm^2$. Radiation length of silica aerogel is $X_0 = 27.25\ g/cm^2$.

2.3.6 Trigger System

(K^-, K^+) events are selected by using trigger system from the event information. The major part of the K^- beams were selected by double mass separation systems prior to the E07 experimental area. To obtain as much as clear (K^-, K^+) events, two types of trigger levels are utilized. The purification of incident K^- beam is getting higher due to the sets of BAC's. The information of incident beam was triggered by using BH1 and BH2 trigger sets.

$$K^- \; beam = BH1 \times BH2 \times \overline{BAC1} \times \overline{BAC2}$$

The signal from the incident beam was rejected by the sets of BAC1 and BAC2. The second trigger system type can be expressed as next:

$$Scattered \; K^+ = PVAC \times \overline{FAC} \times TOF$$

In order to select outgoing K^+ particles, it is required that the particles pass through the TOF wall. From the above, the trigger for selecting the (K^-, K^+) reaction in the E07 experiment is expressed by the next equation:

$$(K^-, K^+) = K^- \; beam \times K^+ \; scattered$$

2.3.7 Target selection

In this analysis polyethylene (CH_2) target run was used to improve the contribution of free protons at the extraction of missing particle. The size of CH_2 is 50[x] $\times$30[y]mm^2 and 30 mm in length is located upstream of the emulsion stack. The density of polyethylene is 2.88 g/cm^2. In the experiment the beam size is expected to be (20[x] $\times$3.2[y]mm^2) under the target location.

Table 2.4: Parameters for the estimation of mom.resolution

Magnetic field	0.72 T
Path length	1.15 m
Momemtum of the incident particles	1.8 GeV/c 1.4 GeV/c 1.8 GeV/c 1.0 GeV/c
DC position resolution	required 200-250 μm
Number of layers	6,4,4 (SDC 1,2,3)
Mass of Kaon (charged $K^{\pm}$)	493.7 MeV/c^2
Mass of pion ($\pi^{\pm}$)	139.6 MeV/c^2

2.3.8 TOF wall

TOF time counters are located at the end of E07 experiment, consist of 24 segments. Figure 2.8 shows the schematic view of TOF wall. And each segment connected with PMT by both sides, up and down PMT. The effective area is $1800mm \times 1800mm$. It was wrapped by aluminised mylar and black sheet to prevent from the cosmic ray. Intrinsic time resolution is about 90 ns.

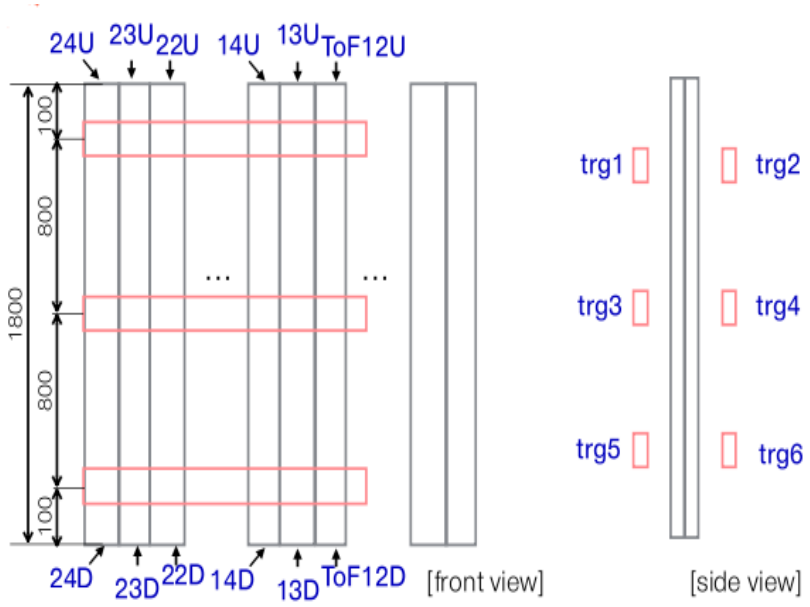

Figure 2.8: The schematic view of TOF wall.

Chapter 3

Analysis

Here we should describe the analysis procedure. The data analysis of the momenum and angle resolutions of kaon, the missing mass analysis of $p(K^-, K^+)\Xi^-$ reaction has been described in details in this chapter. The momentum and angle resolutions of kaon are come from analysis of beamthrough run. In short, for the estimation of momenta and angle analysis,using the data information of K1.8 beam-line spectrometer and the KURAMA spectrometer are in importance. The result of momentum and angle resolutions are applied to estimate missing mass analysis for comparison of data analysis. Since, the missing mass resolution of Ξ^- particle is investigated by utilizing polyethylene (CH_2) target run. In brief, analysis consists of several steps, selection of incident beam K^-, identification of the scattered K^+ by using KURAMA sets, and finally show the missing mass resolution of Ξ hyperon. In addition, for the comparison we made calculation of each resolutions. For the estimating momentum resolution the position resolution of drift chambers and multiple scattering are in crucial. Also we calculated the small scattering angle of each devices and compared with data analysis. Also in this chapter contains the drift chamber (SDC1-2-3) analysis. In SDC's analysis, the angle slope of the x- and y-position has been showed.

3.1 Incident Beam

3.1.1 Incident beam particles

The incident beam is consists of the mixture of kaon,pion and protons as the beam particles. Beam particles are identified by time-of-flight information which was measured by time trigger counters,with BH1 and BH2, respectively. The distance between BH1 and BH2 was around 10.334 m.Figure 3.1 depicts the clear separation of K^- and π^- beam particles. For an incident particles, K^- was chosen. The timing resolution was around 150-160 ps for Kaon. We can see that from the figure 3.1, not only the flight time distribu-

tution of the K^- can be seen, but also the pion- particle's contamination is observable from the plot. We apply the trigger cut condition for each particle type to obtain the clearance of either K^- or π^- as much as possible.

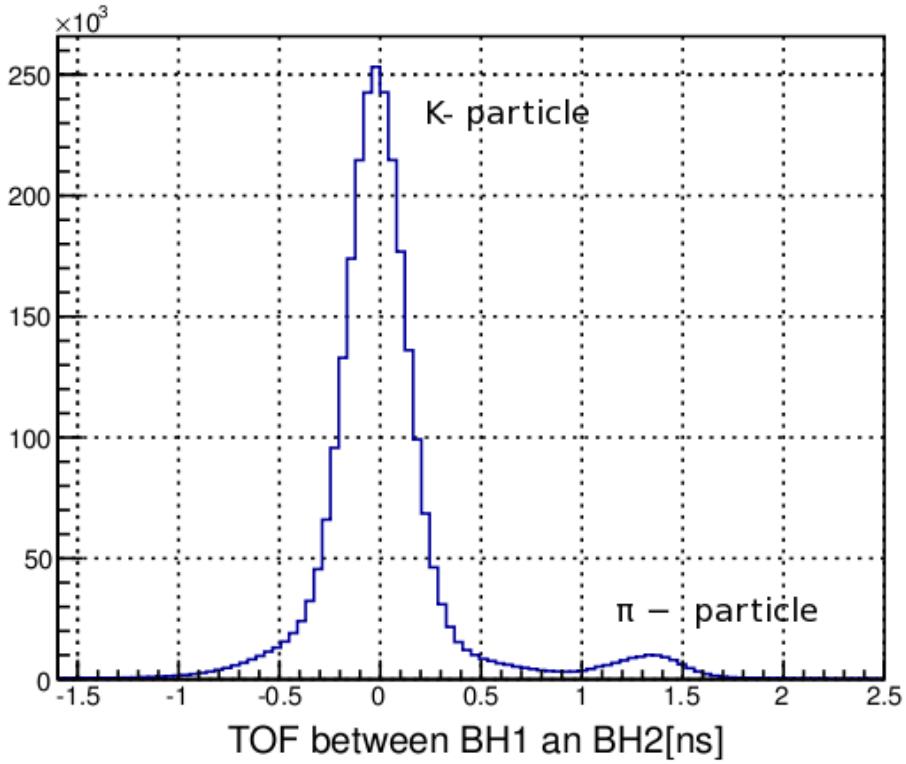

Figure 3.1: Time of flight (BH1-BH2) of beam particles.

3.1.2 Incident beam momentum

The set of magnets in the E07 experiment, namely $Q10$, $Q11$, $D4$, $Q12$ and $Q13$, are used as the beam spectrometer. The upstream track was reconstructed using the chambers BC3-4 and they are located between $Q13$ and BH2. In this analysis expected the dispersion of the incident beam momentum is $\sim 0.01 GeV/c$. The incident beam momentum of K^- was 1.8 GeV/c for the missing mass of Ξ-particle. At the beginning, protons are negligible due to the double ESS system. By setting up trigger condition we can obtain pure K^- beam with the ratio of K^-/π^- to be less than 6. In this analysis we have selected the incoming K^- beam owing to the TOF information. Figure 3.2 displays the incident Kaon beam momentum spread at the K1.8 beam-line. According to plot, the incident beam momentum was for K^- around 1.8 GeV/c at the K1.8 beamline spaectrometer.

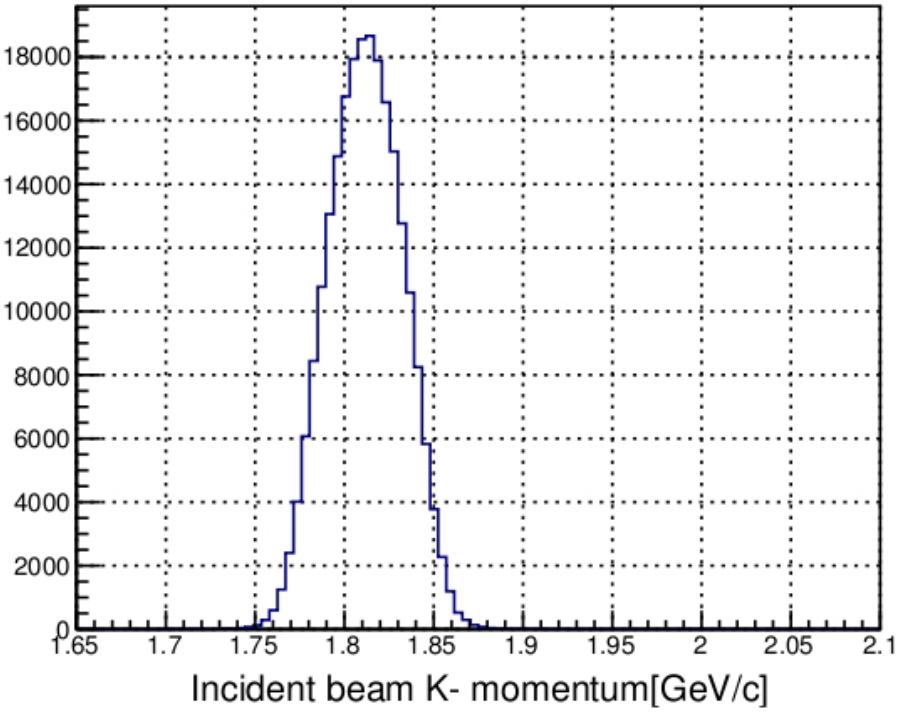

Figure 3.2: The distribution of beam momenta at K1.8 beam-line.

3.1.3 Reaction vertex

The determination of the reaction vertex is investigated from the closest distance between K1.8 track(BcOut) and the KURAMA spectrometer track. The reaction vertices for the $K^-(p, K^+)\Xi^-$ reaction and closest distance spread are given in the Figure 3.3. In the drawing, (a),(b) and (c) indicate the x,y and z-vertex distribution, respectively, (d) represents the closest distance's distribution. The applied angle reaction for those distributions to be settled up between 2°and 20°. Polyethylene target size is 50[x] $\times$ 30[y] mm^2. Therefore the cut condition is attached to have -25 to 25 mm for x- and -15 to 15 mm for y-vertex in conformity with the target size. For the z-vertex cut selection was from -100 to 100 mm. Figure (d) displays the closest distance between the BcOut track and the KURAMA track. In the event case, less than 10 mm was taken as small distance for the closest distance to get good events.

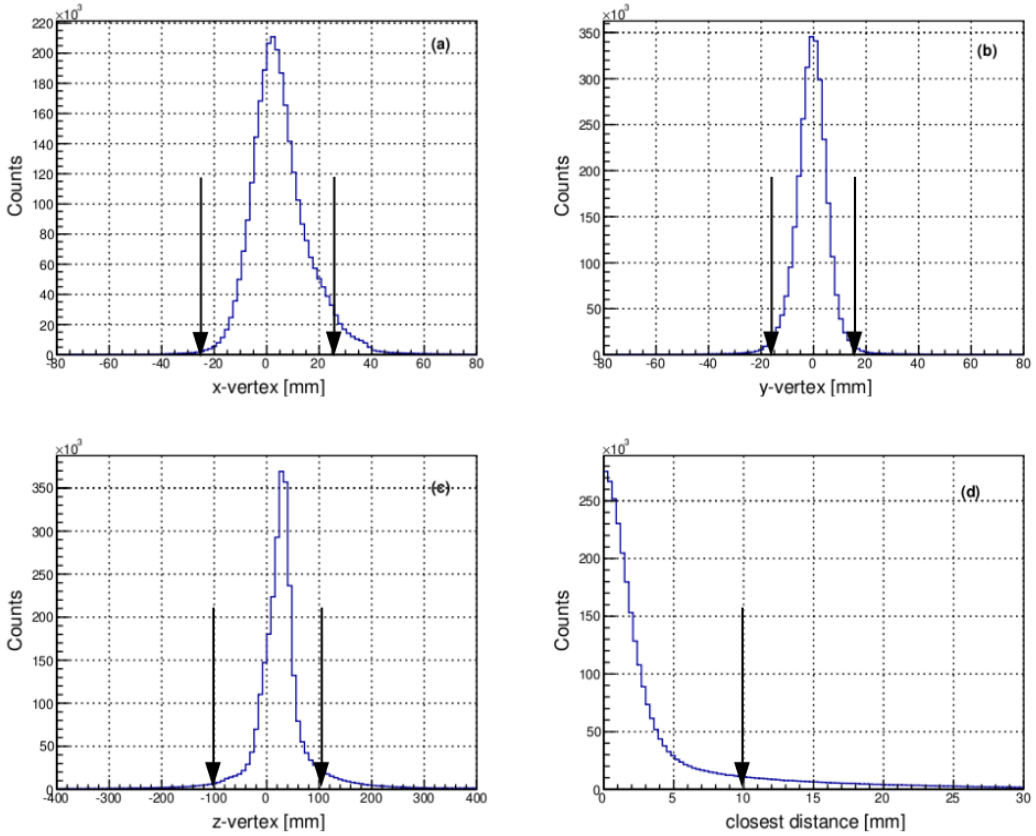

Figure 3.3: Figure (a),(b) and (c) depict the x,y and z-vertex distribution, respectively. Figure (d) represents the closest distance's distribution.

$\chi^2 KURAMA$

Figure 3.4 shows the χ^2 distribution of the KURAMA tracking. In a case of multi-hit events, all tracks between SDCin and SDCout tracks are investigated by the χ^2 values. As an assumption good tracks are belong to less than 20 of χ^2 distribution.

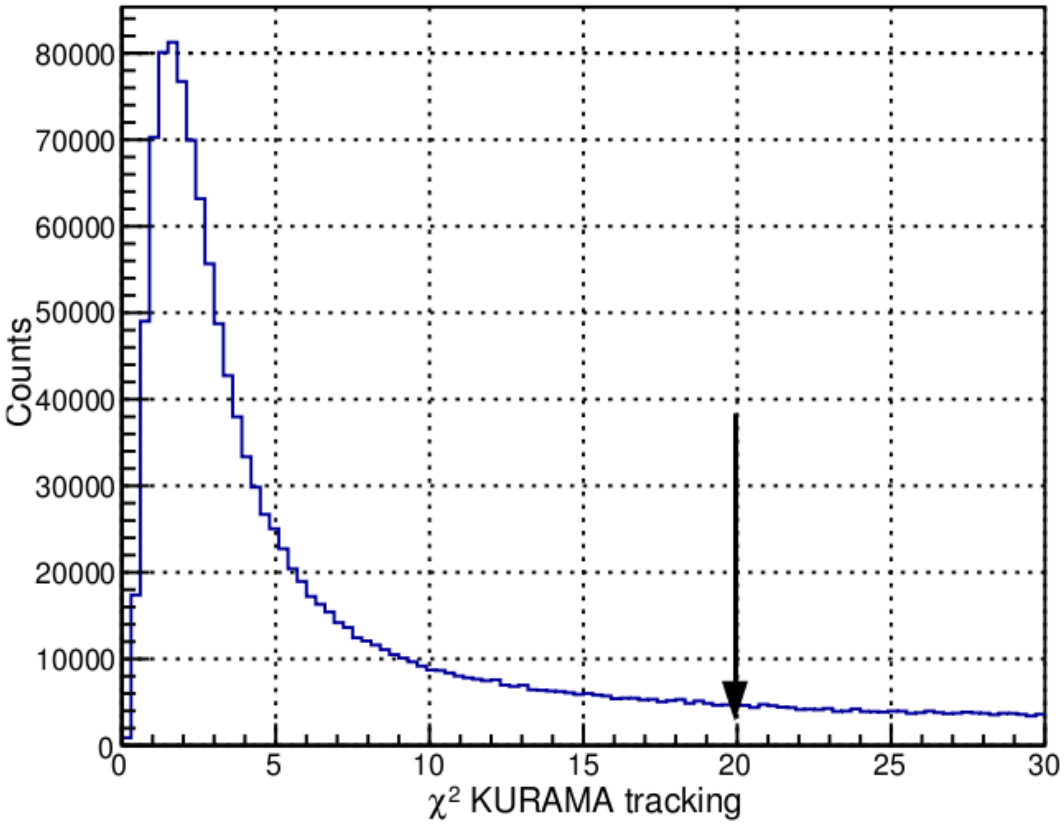

Figure 3.4: The χ^2 distribution of the KURAMA tracking from polyethylene target.As an assumption, good tracks are in the less than 20 for the χ^2 KURAMA track.

3.2 Outgoing K^+ analysis

3.2.1 Mass square of K^+

The determination of the scattered K^+ is significant for the missing mass analysis. Moreover, flight time information of outgoing particles is necessary for the particle identification. Flight time can be gotten from the distance of two scintillator counters,namely BH2 and TOF wall, which is located at the end of KURAMA spectrometer sets. Thus, flight path and momentum of scattered particle's are available, the mass square of outgoing particles is defined by:

$$M^2 = \frac{p^2}{\beta^2}(1-\beta^2) \tag{3.1}$$

where, β - velocity of outgoing particles,

$$\beta = \frac{L}{c \cdot t_{TOF}} \tag{3.2}$$

p -is the momentum of the outgoing particle. L is the distance between BH2 and TOF wall, whereas t_{TOF}-flight time of BH2-TOF wall. Figure 3.5 depicts the momenum and mass correlation plot of the scattered particles. From the drawing, momenta of outgoing K^+ particles is to be below the ranges of 1.4 GeV/c in the Y-axis.

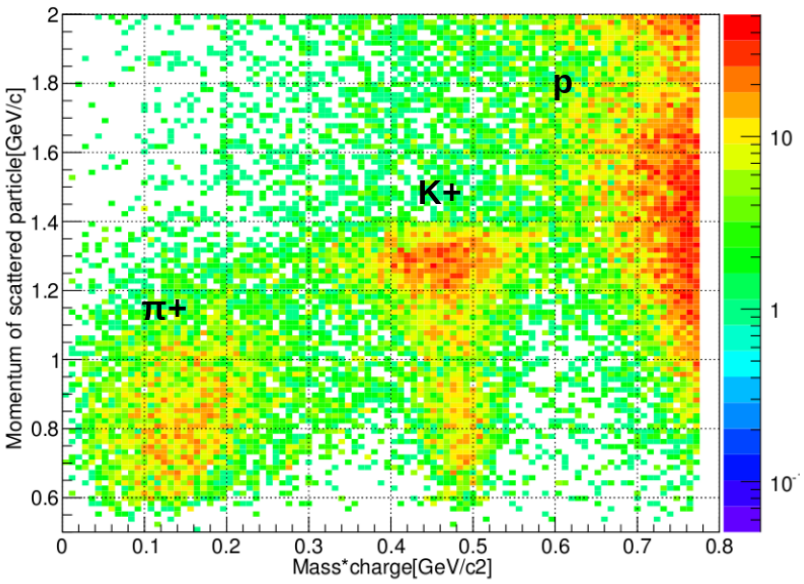

Figure 3.5: Mass vs momentum correlation draw of scattered particles.

3.2.2 Identification of Kaon

Particle identification of the scattered K^+ is defined by the mass of the scattered particles. The mass square distributions are available in the figure 3.6. The plot was gotten out from the poluethylene (CH_2) target run. for obtain the mass square, we applied χ^2 cut to be less than 20 and cut condition of scattered momentum range was from 1.0 to 1.5 GeV/c. Also vertex cuts are applied to obtain (mentioned before) for the identification of scattered kaon. One can see the the peak of π^+, K^+ and proton mass square and scattered kaon's mass has a range around 0.1-0.3 in the Gev/c^2 scale. Therefore, the next attempt is to obtain the momentum of Kaon. As we are looking for the momentum of the scattered

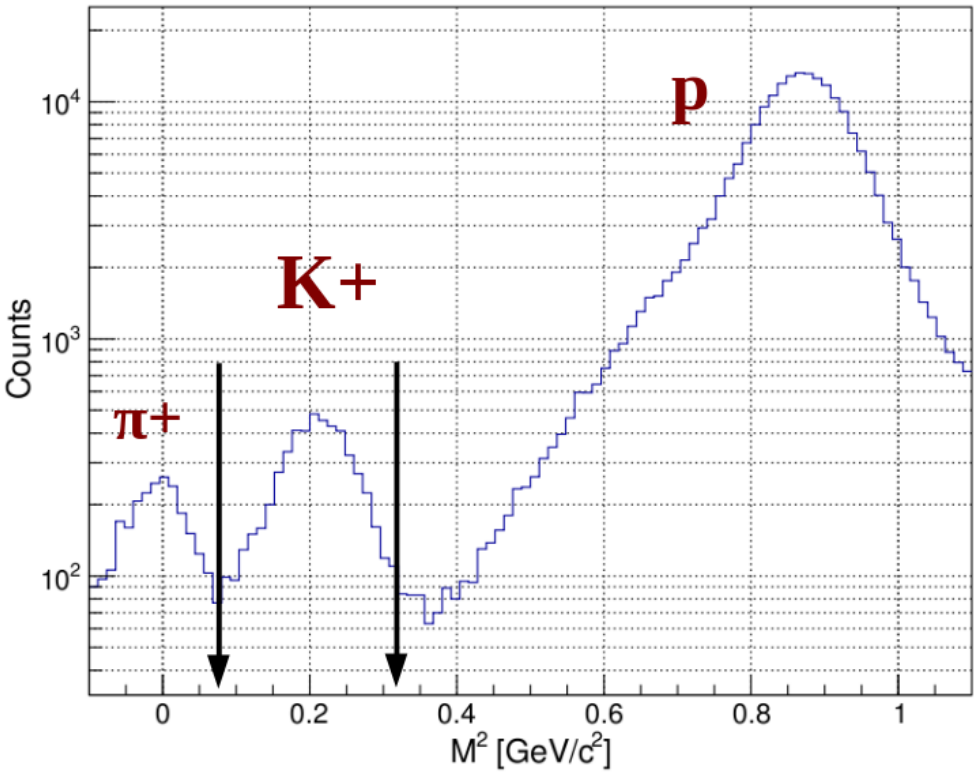

Figure 3.6: The mass square distribution from the CH_2 target run.

Kaon, in accordance with the figure 3.6, the typical momentum for outgoing K^+ is having a range below ~1.4 GeV/c at the beam momentum of 1.8 Gev/c on the CH_2 run. Also we can see the momentum of the largest peak of scattered K^+ particle is belong around $\sim 1.3 GeV/c$. Therefore, χ^2 cut is applied to see the clear peak of outgoing momenta. χ^2 cut is defined to be less than 20 from the Kurama track. And, Figure 3.7 represents the

clear $K+$ peak as expected momentum is around 1.3 GeV/c. The applied cut ranges are defined to have around 1.0 - 1.5 from the momentum distribution of outgoing kaon. After applying cut condition of (1.0-1.5 GeV/c for K^+), as an assumption, with this range of scattered momentum, the Ξ^- particle has been generated.

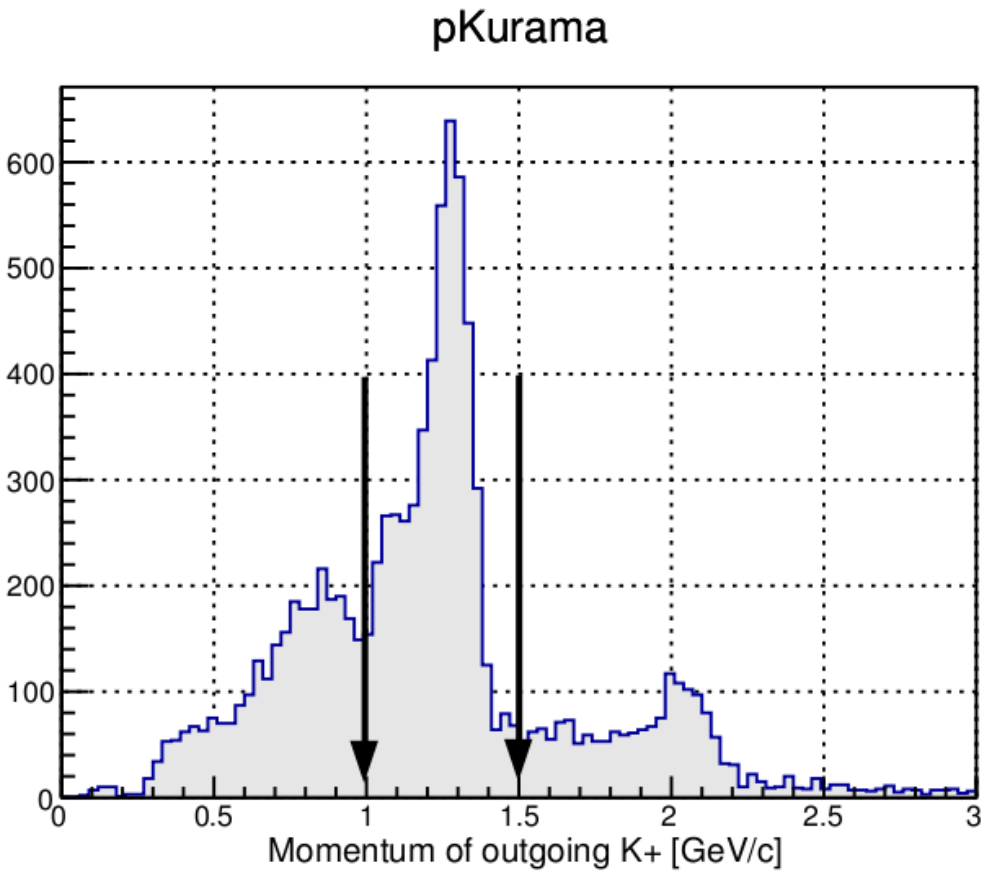

Figure 3.7: The scattered K^+ particle's momentum. In cut region is defined less than 20 for χ^2 from KURAMA track. The applied cut momentum regions are shown by arrow.

3.2.3 Scattered K^+ angle

Figure 3.8 displays the scattering angle of scattered K^+. Cut condition for the theta has to be determined from 2°to 20°.

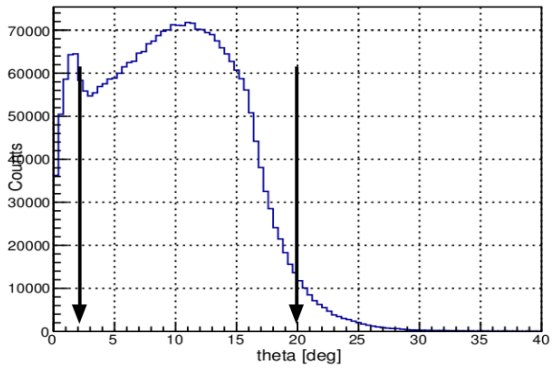

Figure 3.8: The scattering angle of K^+. Cut condition is defined to have a range 2°- 20°.

3.3 Momentum resolution

Before starting analysis procedure, we should clarify the way of how to evaluate the momentum resolution. The momentum analysis was done by taking of kaon particles in the E07 experiment. Data details are given in table 3.1.

Data	Beam mom.(GeV/c)	target
E07	1.0,1.2,1.4,1.8	empty

Table 3.1: Beam through data in the E07.

In the analysis, incoming and outgoing particles are the same. In this paragraph we estimate the momentum resolutions of the KURAMA spectrometer. For the the estimation the difference between momenta of KURAMA spectrometer and K1.8 beam-line momenta are needed. Therefore, at first we should check the momenta distribution of each beam momenta. One can see the beam momenta spread of K1.8 beam-line in figure 3.9 with different momenta values. Looking at the plot we can see the clear peak at around 1.8,1.4,1.2 and 1.0 for K1.8 beam-line. Also it is important to see measured momenta with the KURAMA, which in figure 3.10.
Assuming, the momentum resolution of K1.8 beam-line is expected to be better than $\sim 22 \cdot 10^{-3} MeV/c$, while it is worse than $\sim 10^{-}$in the KURAMA magnet. That's why checking substructed $\Delta p = p_{KURAMA} - p_{K1.8}$ is an importance. The Figure 3.11 displays the Δp of 1.8,1.4,1.2 and 1.0 GeV/c of beam momenta. The resolution of the measured momentum in the magnet is proportional inversely to the bending angle by the magnet. Then angular resolution is determined by the intrinsic angle of drift chambers, in turn intrinsic angle can be expressed with the position resolution of chambers.

After checking the momenta of K1.8 and KURAMA spreading, we can evaluate Δp from the $\Delta p = p_{KURAMA} - p_{K1.8}$ relation. After the substruction, the *gaus* fit function is applied to see the dispersion of the momentum. After analysis, the momentum resolution was 25.2 ± 0.1, 18.43 ± 0.05, 15.32 ± 0.05 and 12.87 ± 0.03 (MeV/c) in $\sigma(sigma)$ for the range of 4 momenta, namely, 1.8,1.4,1.2 and 1.0 GeV/c respectively, seen in Figure 3.11.

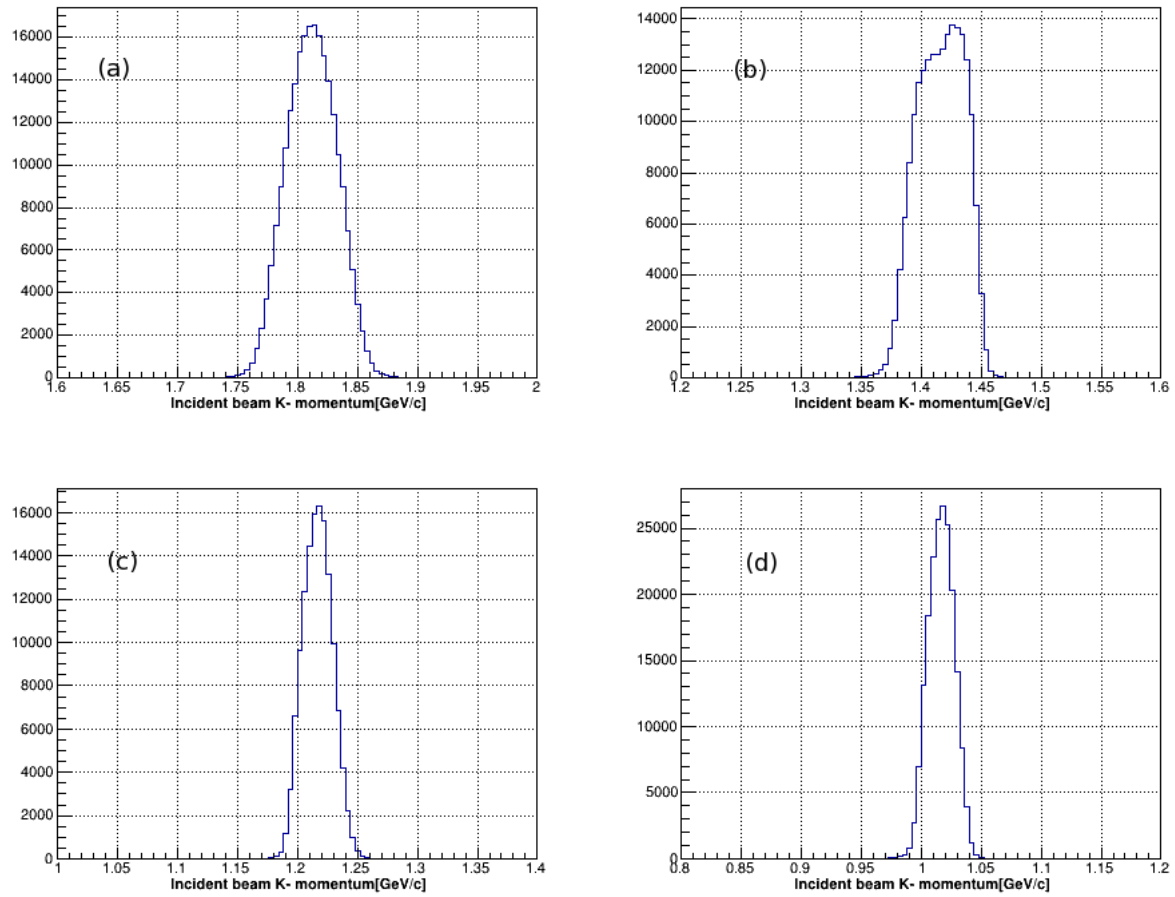

Figure 3.9: Incident beam momentum distribution: (a) 1.8 GeV/c (b) 1.4 GeV/c (c) 1.2 GeV/c (d) 1.0 GeV/c.

After taking Δp, it is important to see the correlation between Δp and initial beam momenta. Figure 3.12 shows the momentum distribution as a function of beam momentum. The plot was drafted from kaon particles analysis. By increasing momentum (from 1.0 to 1.8 GeV/c) the momentum resolution rises up as plot says. By assumption, Δp has a major contribution of position resolution from the tracking detectors. The reason of increasing the momentum resolution is belongs to the next relation: $\frac{\Delta p}{p} \propto p$. According to attitude of Δp *and* p, the momentum resolution increases by maximizing momenta.

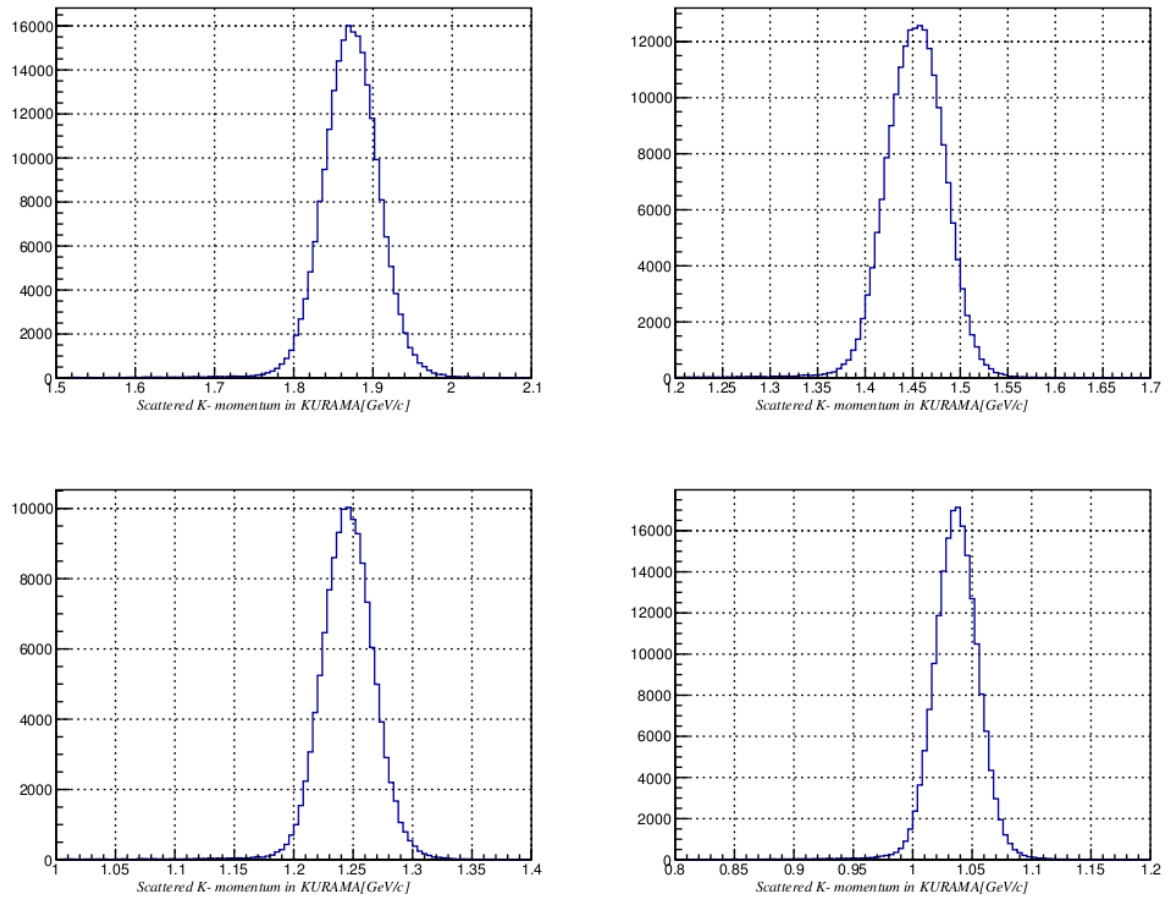

Figure 3.10: Beam momentum distribution in the KURAMA magnetic field.(a) 1.8 GeV/c (b) 1.4 GeV/c (c) 1.2 GeV/c (d) 1.0 GeV/c.

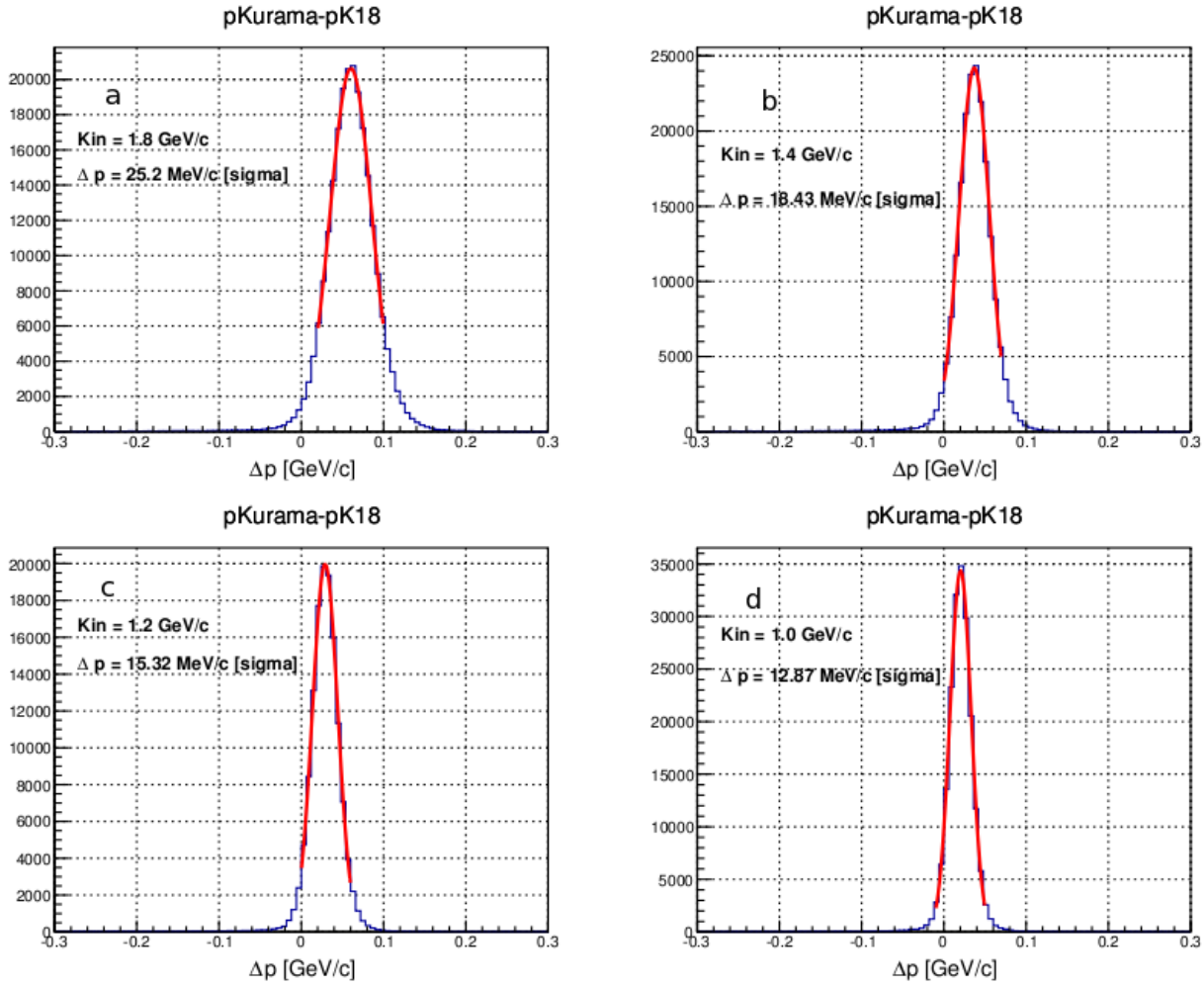

Figure 3.11: Δp distribution with fitting:(a) 1.8 GeV/c (b) 1.4 GeV/c (c) 1.2 GeV/c (d) 1.0 GeV/c.

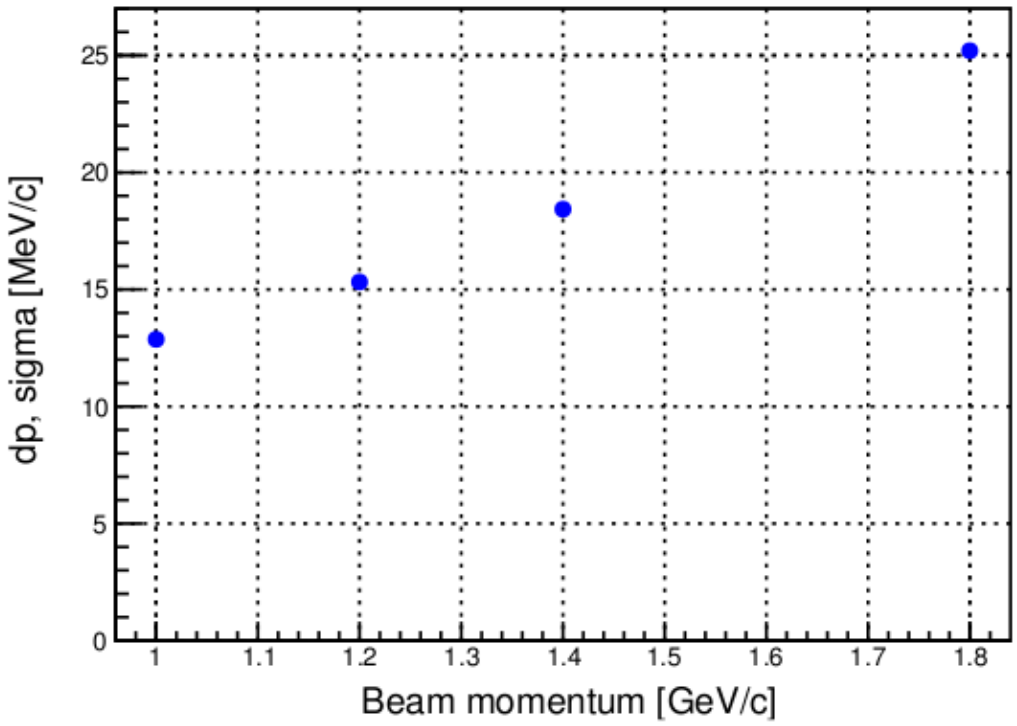

Figure 3.12: The Δp distributiion as a function of beam momentum.

3.4 Angular resolution

Scattered particles are defined with the KURAMA magnet and the sets of drift chambers. The bending angle is defined from SDCin and SDCout, so $\theta = \theta_{SDCout} - \theta_{SDCin}$. This analysis method usually calls construction of the local track. There 4 parameters at beginning to define:

- x - horizontal position,
- y - vertical position,
- u - dx/dz angle slope from x axis respect to z position,
- v - dy/dz angle slope from y axis respect to z position.

The scattered particle's angle before KURAMA magnet is determined with the SDC1, which located at the entrance of magnet. Ususally it calls SDCin tracking. Outgoing particles track after KURAMA magnet are determined with SDC 2-3 two chambers, totally call them together SDCout.

SDCin analysis

Usually, we deal with slope of $u(dx/dz)$ and $v(dy/dz)$ angle, because entered particles are tend to change their path not only by x-position,but also by y-position. One can see the angle distribution of u and v from SDCin in figure 3.13.

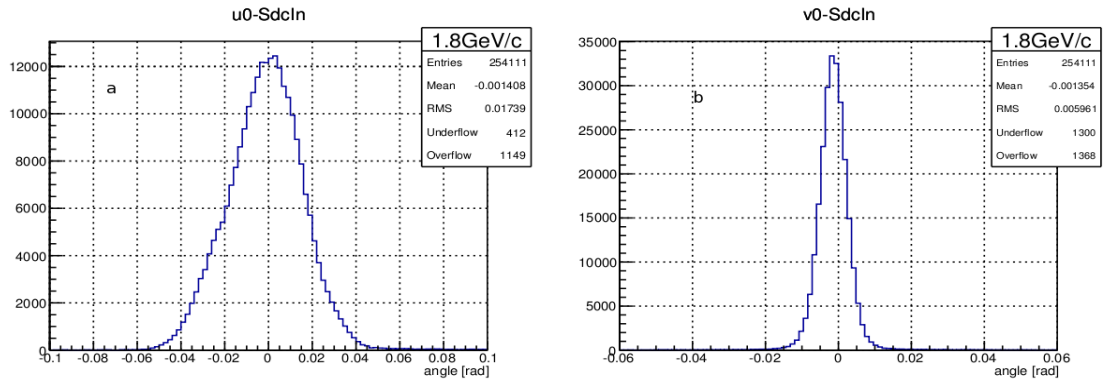

Figure 3.13: $u(dx/dz)$[a] and $v(dy/dz)$[b] angle distribution of SDCin at the 1.8 GeV/c beam momentum.

SDCout analysis

By the SDCout analysis,one can see the distribution of the u and v planes in figure 3.14. After the substruction of angle from SDCin and SDCout chambers, we can estimate the angle resolution of KURAMA spectrometer by fitting *gaussian*. In the current fit says from figure 3.15, the angle resolution is around 2.8 mrad both dv and du, along y- and x-axis respectively, at the 1.8 GeV/c initial momentum.

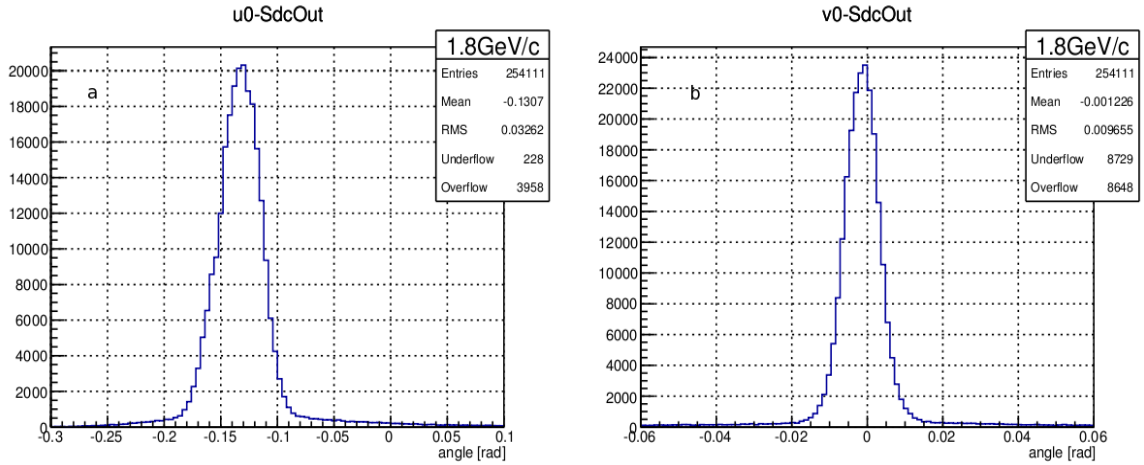

Figure 3.14: $u(dx/dz)$[a] and $v(dy/dz)$[b] angle distribution of SDCout at the 1.8 GeV/c beam momentum.

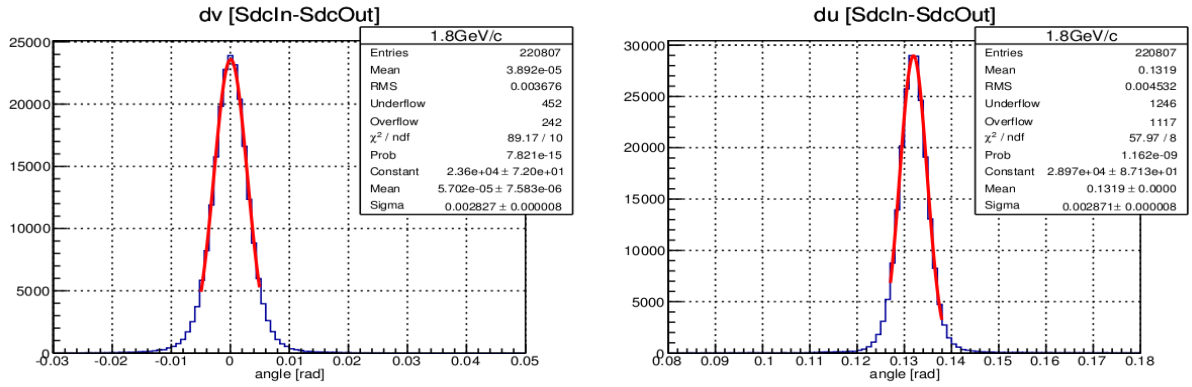

Figure 3.15: The angle distribution [rad], (a)dv and (b)du, at the 1.8 GeV/c incident beam.

Multiple scattering angle

The analysis was done for small scattering angle by taking tracks of before and after target position. The Figures 3.16 and 3.17 represent the small scattering angle substraction of before and after target position respect to u and v angles, which comes from along with x and y directions. After substracting 2 systems, we fit the *gaus* to receive the resolution of small angle. Also, it is easy to notice that angle distributions are getting narrower with increasing momentum for both du and dv distributions, figures 3.19 and 3.20. After fitting, σ_{du} was 0.003095, 0.004047 ,0.00465 and 0.00576 rad for momentum of 1.8,1.4,1.2 and 1.0 GeV/c,respectively. Moreover, σ_{dv} was 0.003606,0.004568,0.005234 and 0.006399 in rad for the initial beam momentum, respectively. Comparison of data and calculation are described in the result section.

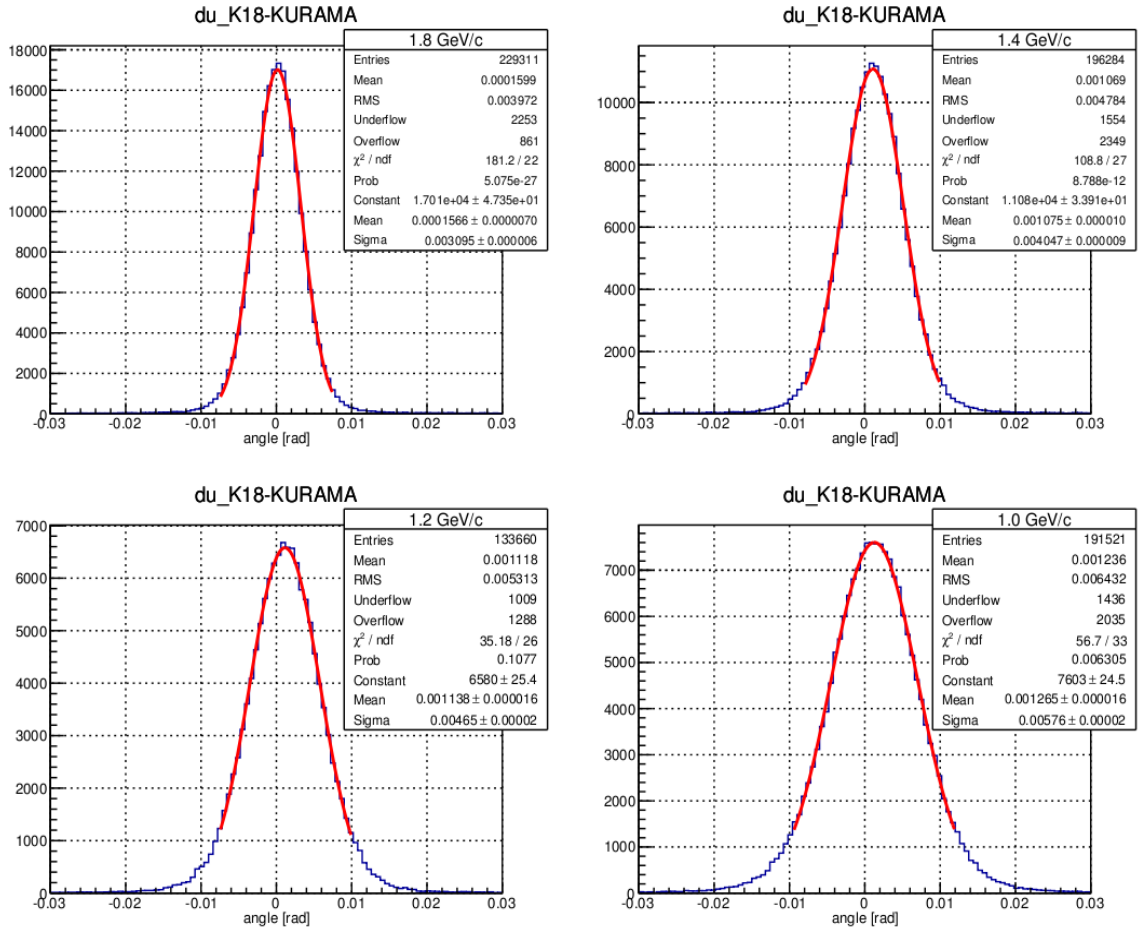

Figure 3.16: du angle distribution, along with x axis at the 4 momentum: (a) 1.8 GeV/c (b) 1.4 GeV/c (c) 1.2 GeV/c (d) 1.0 GeV/c

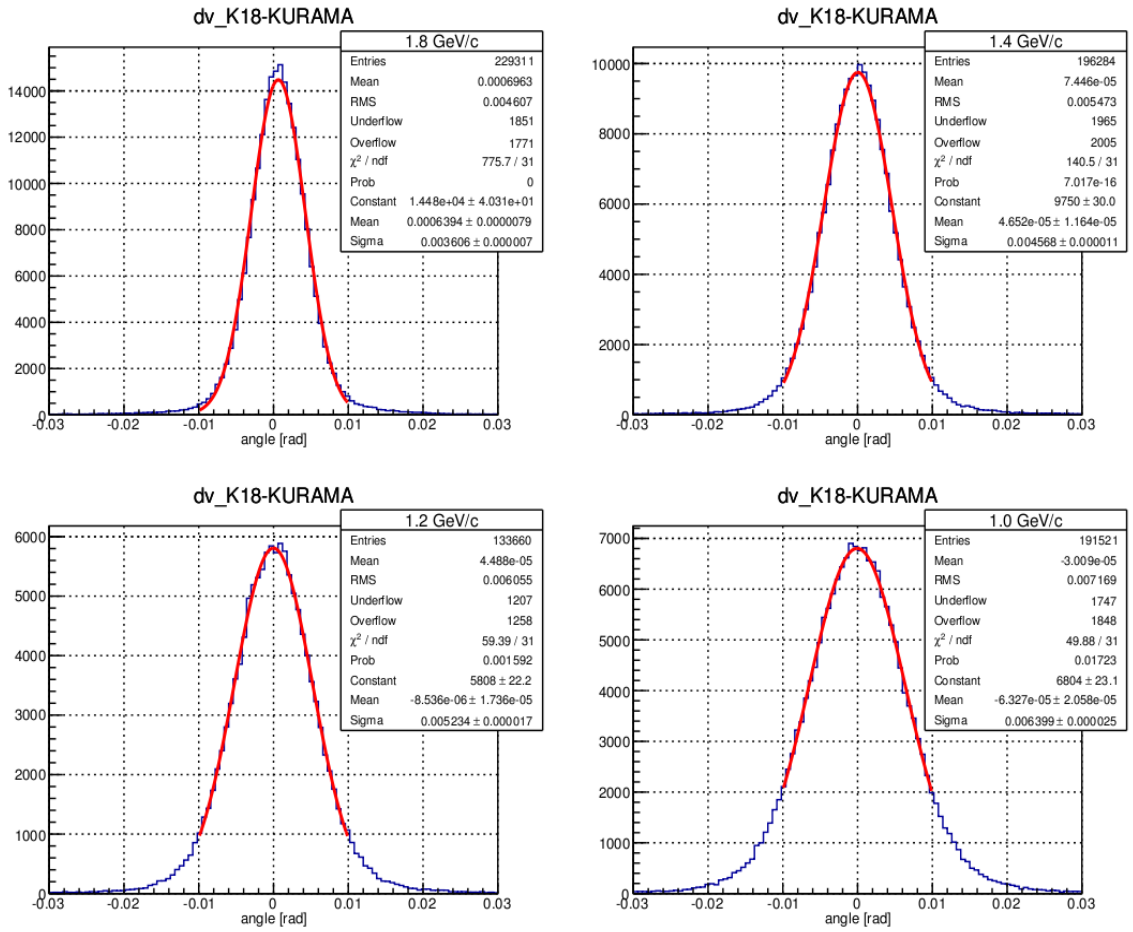

Figure 3.17: *dv* angle distribution, along with y axis at the 4 momentum: (a) 1.8 GeV/c (b) 1.4 GeV/c (c) 1.2 GeV/c (d) 1.0 GeV/c

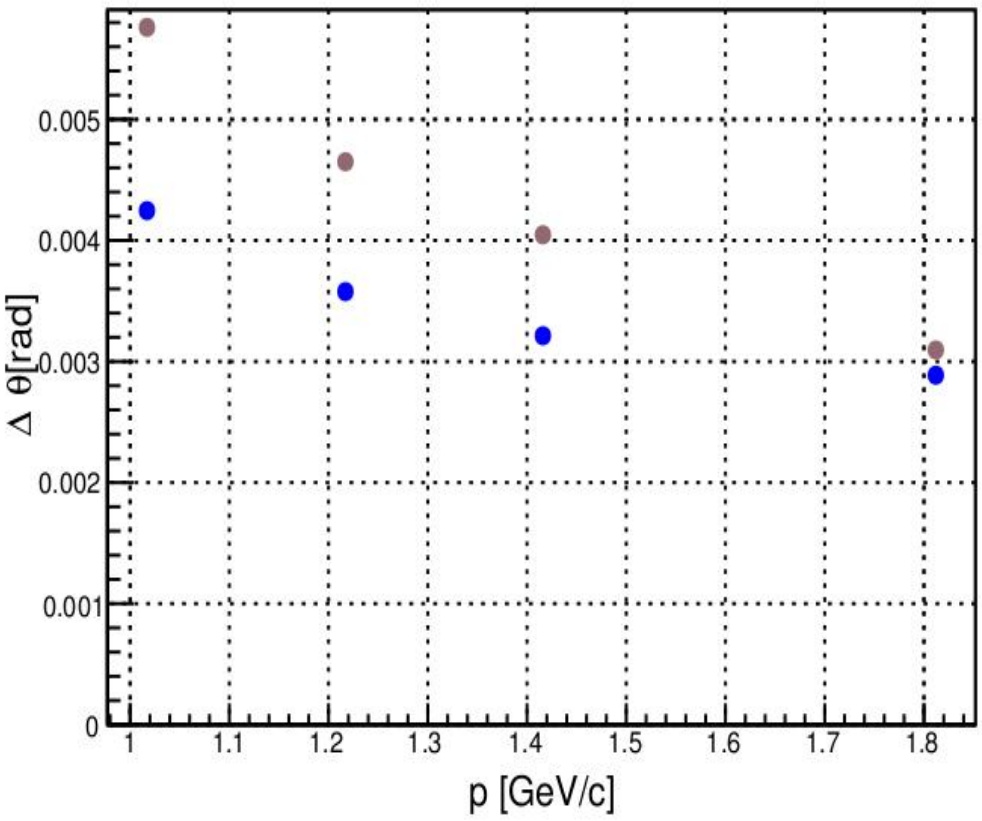

Figure 3.18: $\Delta\theta$ as a function of beam momentum.

In figure 3.18, the angle resolution are drafted respect to beam momentum. It is easy to notice that with increasing beam momentum, angle resolution gets smaller. At first we clarify the mean dots, *"grey"* dot comes from K1.8-KURAMA track subtraction at the target position, while *"blue"* is for KURAMA spectrometer system. $\Delta\theta$ from both system is decreasing by maximizing momenta. The main reason could be the following attitude: $\Delta\theta \propto \frac{1}{p}$.

3.5 Kinematics of Missing Mass

The missing mass which is the mass cannot measured directly. Missing mass is obtained by the measurement of the conversation of the momentum of incoming and outgoing particles. At first, we should give the clarification of formula of 3 vector momenta of the incoming K^-, the outgoing K^+, the target and missing particle momenta after the $K^- + p \Rightarrow K^+ + \Xi^-$ reaction. According to the energy and momentum conservation, the sums of the 3 vector momenta are identical. According to momentum conservation law, the next relation according to kinematics:

$$\vec{P_{K-}} + \vec{P_{tgt}} = \vec{P_{K+}} + \vec{P_x} \tag{3.3}$$

then,

$$\vec{P_x} = \vec{P_{K-}} + \vec{P_{tgt}} - \vec{P_{K+}} \tag{3.4}$$

$$E_{K-} + E_{tgt} = E_{K+} + E_x \tag{3.5}$$

thus,the missing mass can be expressed as below,

$$M_x = \sqrt{(E_{K-} + M_{tgt} - E_{K+})^2 - (p_{K-}^2 + p_{K+}^2 - 2p_{K-}p_{K+}cos(\theta_{K^-K^+})} \tag{3.6}$$

where E_{K-} and E_{K+} -are the total energy of incoming and outgoing kaons, M_{tgt} - the target mass, $\theta_{K^-K^+}$ - the reaction angle. From taking momentum and energy conservation of incoming and outgoing particles, one can calculate the missing mass of uncertain particle's from the reaction.

3.6 Missing mass

Before identifying the missing mass spectrum, from the previous analysis reliable cut conditions are applied to obtain the missing mass distribution. The missing mass spectrum was given in the figure 3.19. The plot was taken from using CH_2 target run in the E07 experiment. The Ξ^- mass in the Particle Data Group (PDG)[14] is $1321.71 \pm 0.07 MeV/c^2$.

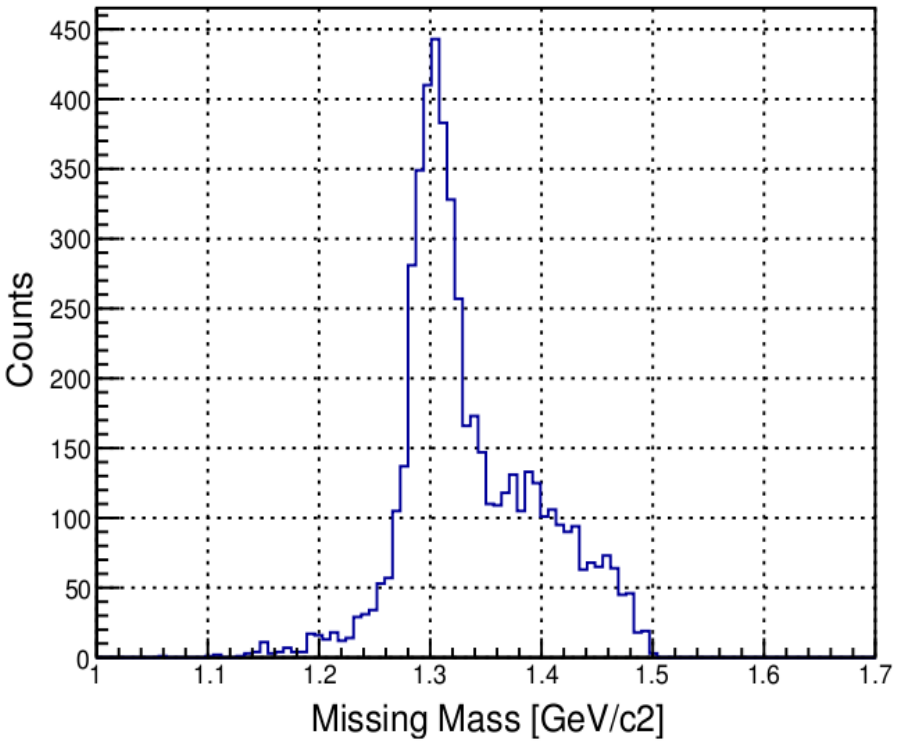

Figure 3.19: The missing mass spectrum of Ξ^- received from the CH_2 target run in the E07 experiment.

Correction for missing mass

Principally, in the KURAMA spectrometer system, there is a no relation between the mass and the scattering angle. However, for considering correction, we show the missing mass as a function of with x and y-positions, a horizontal u (dx/dz) and a vertical v (dy/dz) angles of KURAMA. Figure 3.20 displays missing mass with, x and y positions, a horizontal and a vertical angles of the KURAMA track. From the plot the relation of missing mass

and u angle is clear, while from other correlations missing mass contributions almost insignificant. In further analysis we should correct line to be straight respect to u angle which is $\frac{dx}{dz}$ angle by x-axis according to scattered particle's path.

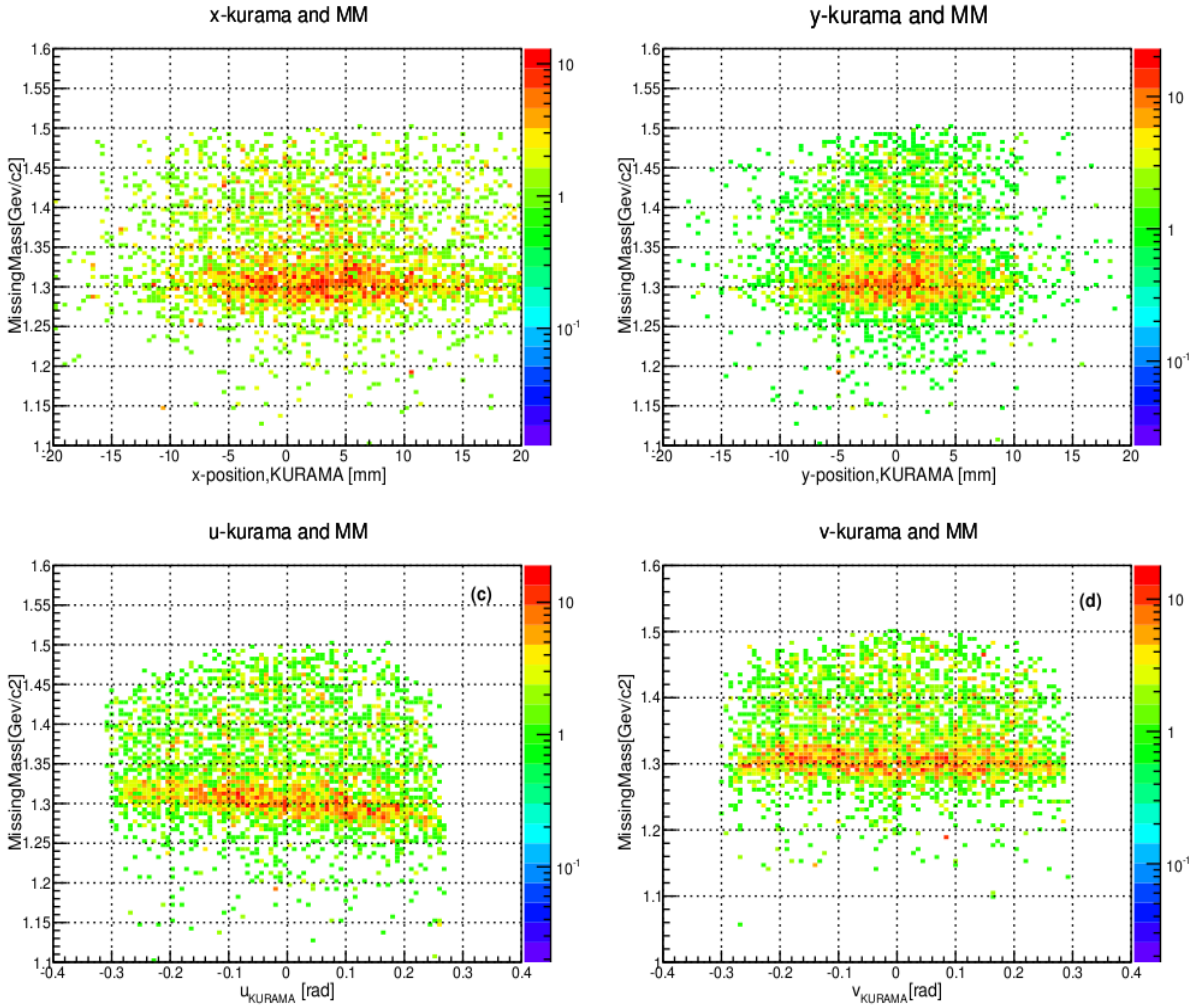

Figure 3.20: Correlation plots of missing mass with, (a)x position, (b) y position, (c) a horizontal and (d) a vertical angles of the KURAMA track.

As we mentioned before relation between mass and angle by x-axis of KURAMA is clear, it means the correction procedure is needed. The figure 3.21 represents how we made correction to missing mass respect to u angle. So,MM_{corr} defined as

$$MM_{corr} = MM + X \cdot u$$

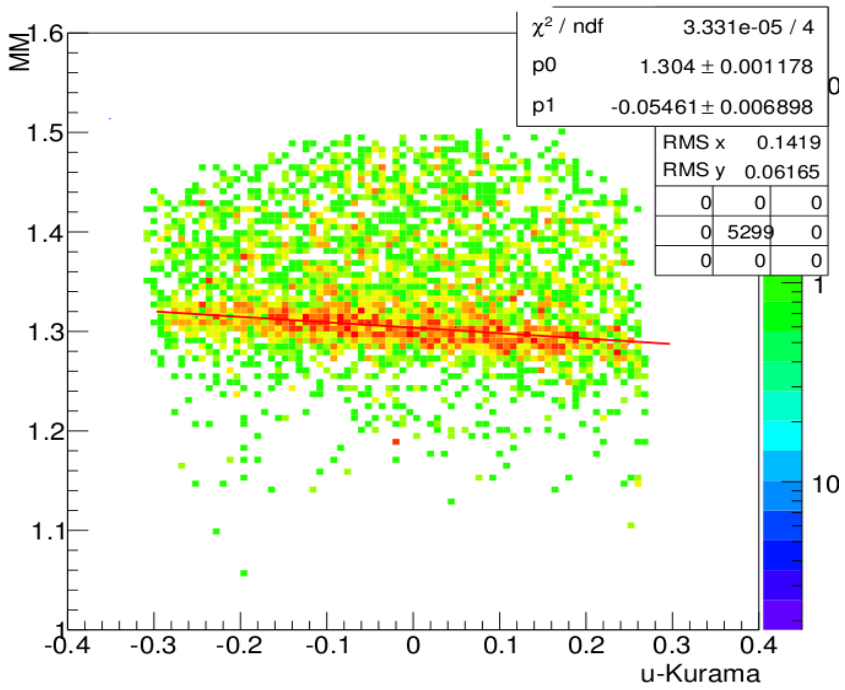

Figure 3.21: Correction to missing mass with angle u KURAMA.

where, X - correction factor, slope of the line. After application of correction factor (X=0.05461±0.006898), the result is given in the figure 3.22. We can see the slope gets to have straight line after correction.

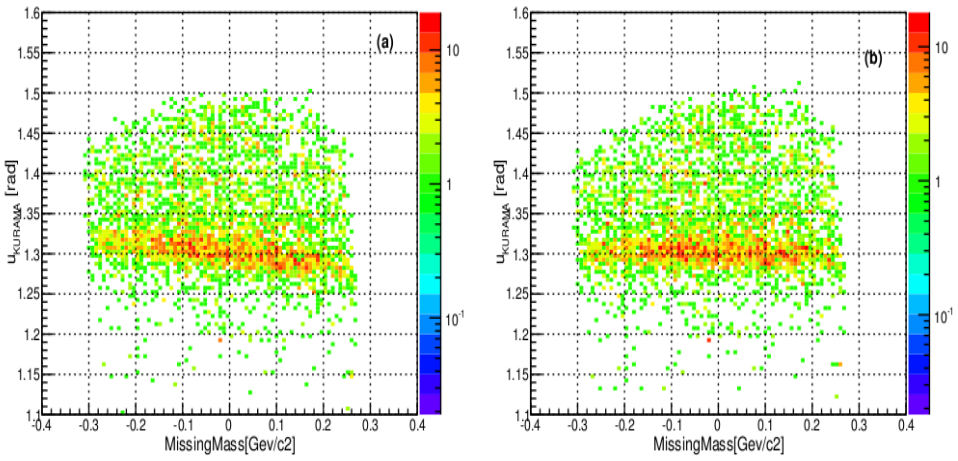

Figure 3.22: Missing mass vs $\frac{dx}{dz}$-angle. (a)-not corrected, (b)-corrected.

It is better to see the missing mass distribution after with fitting gaussian. Figure 3.23 reveals the missing mass distribution before and after correction. It is easy to catch out looking at the graph, that after missing mass width getting narrower. Before correction, the missing mass resolution is about 19.92 ± 0.64 $[\sigma] MeV/c^2$, while after correction total fit was around 15.76 ± 0.38 $[\sigma] MeV/c^2$. The result is important because in further it will be compared with the calculation.

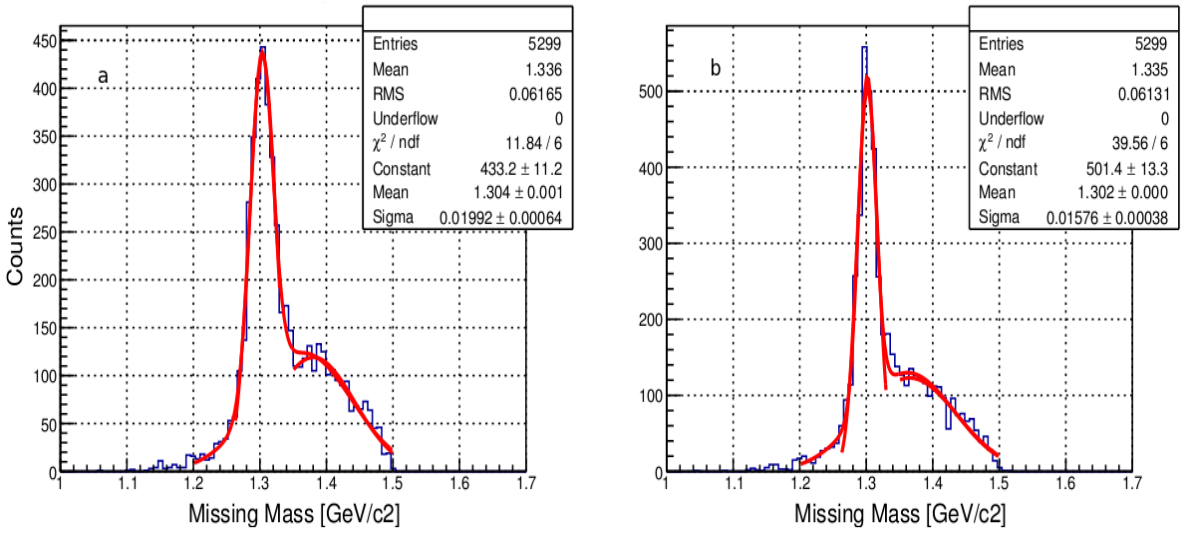

Figure 3.23: The missing mass distribution: (a)before, (b)after correction by angle.

Chapter 4

Results and Disscussion

In this chaptep contains the theoretical estimation of the momentum and angle resolutions of kaons of beamthrough analysis. Momentum resolution has been affected by the position resolution of Drift Chambers and multiple scattering effect. We will see this dependence in further into this chapter. The missing mass calculation will be done by taking the assumptions which based on the momentum and angle analysis. Also the comparison will be made up with the analysis result and theoretical calculation.

Momentum resolution

Through the strong magnetic field, the momenta of charged particles can be defined. Owing to the effect of the Lorentz power particles are believed to follow circular orbit that may be assessed by the kits of multi-wire drift chambers which located before-after the KURAMA dipole magnet. Usually *magnetic spectrometers* are utilised to define the particle's trajectory which goes through the magnetic pole. With the help of the magnetic field the bending angle is calculated. As an assumption of the next $\delta p/p \propto p$, the particle's path is tend to be straighter with the magnification of strong momenta [1].
The momentum

$$p = 0.3 \cdot B \cdot R[\frac{GeV/c}{Tm}] \tag{4.1}$$

- *B – strength of magnetic field (KURAMA) [T]*
- *R – radius of curvature [m]*

If $L(m)$ - path length and $\theta(rad)$ – bending angle,

$$L \approx \theta \cdot R$$

(4.1) equation becomes,

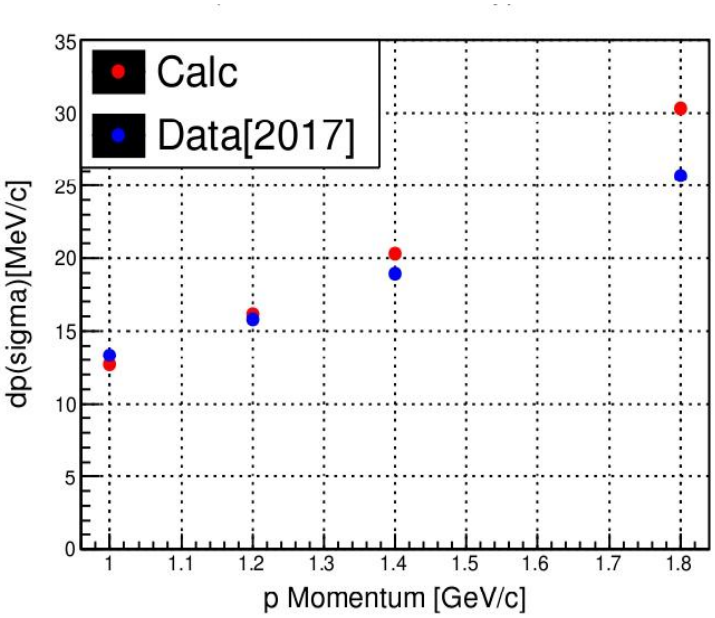

Figure 4.1: Comparison hand and data of momentum resolution(sigma) respect to beam momenta.

$$p \approx 0.3 \cdot B \cdot \frac{L}{\theta} \tag{4.2}$$

If L is not changed, relative accuracy momentum of the measurement defined by the relative angle.

$$\frac{\Delta p}{p} \approx \frac{\Delta \theta}{\theta} \tag{4.3}$$

As seen in figure 4.1, the comparison of calculation and data analysis results of momentum resolution is given. For example, at 1.8 GeV/c case the deviation of data and calculation was $\sim 0,83$, and at 1.0 GeV/c: $\sim 1,05$. According to those magnitudes, we assume that the results are in good agreement.
According to (4.3), the momentum resolution has a inverse relation to the bending angle. Therefore, the next step is the consideration of angles. In this analysis we settled up the length to be $L = 1.15m$. After adjustment of real path length of particles in the KURAMA spectrometer, we have verified it with data results as seen in figure 4.2. In figure 4.2 the ratio of data and calculation results are shown respect to beam momentum. Owing to plot, our adjustment of L is satisfied with the data results. In the data analysis, $\theta = \theta_{out} - \theta_{in}$ - bending angle is determined by the drift chambers, which is located before

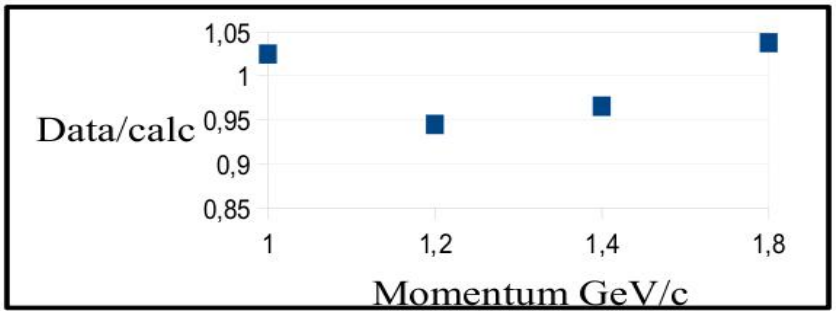

Figure 4.2: Checking bending angle with data.

and after the KURAMA magnet and position resolutions of the drift chambers before and after KURAMA magnetic field.

- θ_{in} from SSD2-SDC1 (before KURAMA)
- θ_{out} from SDC 2-3 (after KURAMA)

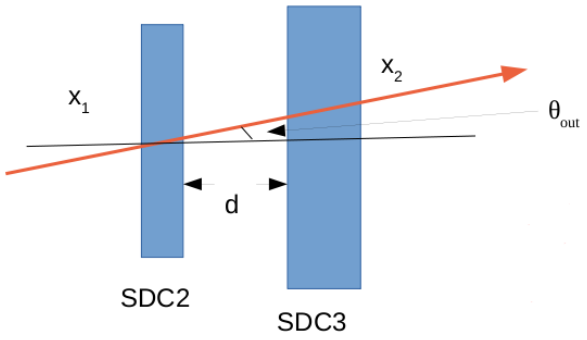

Figure 4.3: A brief image of angle measuring of drift chambers.

In order to evaluate the bending angle resolution, at first we should define the intrinsic angle resolutions of the drift chambers,specifically $\Delta\theta_{in}$ and $\Delta\theta_{out}$. The bending angle resolution can be expressed in terms of drift chamber angle resolutions, so

$$\Delta\theta = \sqrt{\Delta\ \theta_{in}^2 + \Delta\ \theta_{out}^2} \tag{4.4}$$

Figure 4.3 shows the measurement of the angles of drift chambers. The angular resolutions of tracking are estimated with the position resolutions of the chambers.

$$\tan\theta = \frac{x_2 - x_1}{d} \tag{4.5}$$

In order to determine the intrinsic angle resolution of drift chambers, we estimate the intrinsic position resolution of sets of drift chambesr.

$$\Delta\theta = \frac{\sqrt{\Delta {x_1}^2 + \Delta {x_2}^2}}{d} \tag{4.6}$$

$\Delta x's$ are the position resolutions of SSD2-SDC1 and SDC2,3. If position resolution are available, momentum resolution can be expressed:

$$\frac{\Delta p}{p} = \frac{\Delta\theta}{\theta} = \frac{1}{\theta}\sqrt{\frac{\Delta x_{in1}^2 + \Delta x_{in2}^2}{d_{in}^2} + \frac{\Delta x_{out1}^2 + \Delta x_{out2}^2}{d_{out}^2} + \Delta\theta_{multi}^2} \tag{4.7}$$

In a state of estimating the momentum resolution the multiple scatters cannot be ignored so far. Basically, multiple scattering can happen everywhere in the experiment.
High momentum case, the effect of multiple scattering gets smaller by increasing with momentum. According to the next relation:

$$\Delta p = \frac{\Delta\theta}{0.3 \cdot q \cdot B \cdot L} \cdot p^2 \tag{4.8}$$

The relation of Δp and p is clear, so by decresing momenta the multiple scattering contribution gets larger. Therefore the next step is the contribution of the Multiple Scattering via medium.

Multiple scattering through matter

If charged particles, for instance K^- or π^-,traverse the medium are deflefted by small-angle scatters. Most of this scatters can happen due to the Coulomb scattering in nuclei. These Coulomb scattering can be explained by Moliere theory[[5][6]].
The reflection of MS is well described by Moliere distribution:

$$\Delta\theta_{ms} = \frac{13.6[MeV]}{\beta \cdot p \cdot c}\sqrt{\frac{x}{X_0}}\left(1 + 0.038 \ln \frac{x}{X_0}\right) \tag{4.9}$$

Here,

- x - path length
- X_0 - the radiation length of medium (material)
- p- momenta

According to the E07 experiment, a multiple scattering happens by many parts of the experimental equipments. After bombarding the CH_2 target with the incident particle, the MS occurs by each device of before-after the target position. In particular, the multiple scattering are caused by such as PVAC and FAC (aerogel counters), the sets of drift chambers (SDC1-2-3) and others. One point is, not only devices also the MS can be caused by air. Therefore, the angular resolution is the sum up all the system of small scattering angles. Theoretical estimation of MS is computed using equation (4.9). In that case, we use for calculation some constant parameters, such as *radiation length* and *thickness* which provided by the E07 experiment, which are given in table 4.1 and 4.2 for materials.

Table 4.1: Radiation length of material

Radiation length, Argon gas	11760 cm [from PDG,2016]
Radiation length, Air (dry, 1atm)	30390 cm [from PDG,2016]
Radiation length, BH2,FBH,SCH	43.79 cm
Radiation length, BAC1/2, PVAC,FAC	27.25 g/cm2, silica aerogel
Radiation length Ssd1/2	21.82 g/cm2 Silicon (Si)

Table 4.2: Parameters for material

Thickness of SDC1	45.197mm (4.5197 cm)
Thickness of SDC2	32mm (3.2 cm)
Distance between SDC1 and SDC2	255.731 cm
Distance between SDC2 and SDC3	284.0105 mm
Distance between SSD2 and SDC1	383.8425 mm (38.4 cm)
β Kaon [1.8 GeV/c]	0.9645
β Kaon [1.4 GeV/c]	0.9432
β Kaon [1.2 GeV/c]	0.925
β Kaon [1.0 GeV/c]	0.897

Total angular distribution of KURAMA spectrometer:

$$\Delta\theta^2 = \Delta\theta^2_{DC} + \Delta\theta^2_{multi} \tag{4.10}$$

Here, $\Delta\theta_{DC}$-comes from taking into account the position resolutions of tracking detectors,namely the SSD2-SDC1 before the KURAMA and SDC2-3 which is placed after the KURAMA magnet. According to equation (4.10), multiple scattering is calculated for

each devices of in the E07 experiment, namely, around KURAMA spectrometer, they are: PVAC, FAC, SCH, SDC1 and SDC2 (inside argon gas). The Figure 4.4 displays the total angular resolution of the KURAMA spectrometer area. As an assumption, the position resolution has a large contribution for the sum of angle resolution, while multiple scattering partion is minor for angular resolution. Figure 4.4 says that the contributions of total multiple scattering come from FAC, SCH and Air. One thing is important that MS can happen everywhere, it means that angle resolution contains MS of each apparatus ,and also Air contribute to total MS. Table 4.3 represents values of the calculation of angle resolutions in the KURAMA spectrometer system.
In Figure 4.5, the angle resolution of K1.8-KURAMA track is represented. We assume that multiple scattering has a large contribution for K1.8 – KURAMA track at the target position. As can be seen from plot, the contribution of tracking detectors resolution is minor compare with multiple scattering.

Figure 4.5 shows the ratio of data and calculation respect to 4 different beam momentum, namely 1.0,1.2,1.4 and 1.8 GeV/c. The graph provides the information of bending angle, angular resolution (*both dv and du angles*) of KURAMA spectrometer and target position.Due to plot, data and calculation results ratio tend to be around ~ 1.05 on average. Therefore, obtained results are lying within the range of $0.95 \sim 1.13$. Moreover, the reason of the fluctuation of the ranges, mainly comes from the data analysis. And we conclude that our calculation and data analysis results are consistent within this mentioned beam momentum.

p[GeV/c]	1.017	1.217	1.416	1.812
E[GeV]	1.1262	1.311	1.493	1.878
β	0.9004	0.9275	0.9446	0.9654
$\Delta\theta_{DC}$[position resol]	0.00159	0.00159	0.00159	0.00159
PVAC	0.000621	0.000502	0.000425	0.000324
FAC	0.00117	0.000947	0.000801	0.00061
SDC1	0.00039	0.000316	0.000267	0.000203
SCH	0.000826	0.000669	0.000566	0.000431
Air	0.000729	0.00059	0.0005	0.00038
SDC2	0.000322	0.000261	0.000221	0.000168
MS-total	0.00184	0.00145	0.00123	0.000937
TOTAL	0.00239	0.00215	0.00201	0.00184

Table 4.3: Table of the contribution of angle resolution.

Beam momentum [GeV/c]	Δp [MeV/c] Calculation	1^{st} period of E07 exp. Δp [MeV/c]	2^{nd} period of E07 exp. Δp [MeV/c]
1.812	30.32	26.65	25.2
1.416	20.25	20.22	18.43
1.217	16.14	17.68	15.32
1.017	12.7	15.1	12.87

Table 4.4: The momentum resolution: calculation,1^{st} period E07 and 2^{nd} E07 exp.

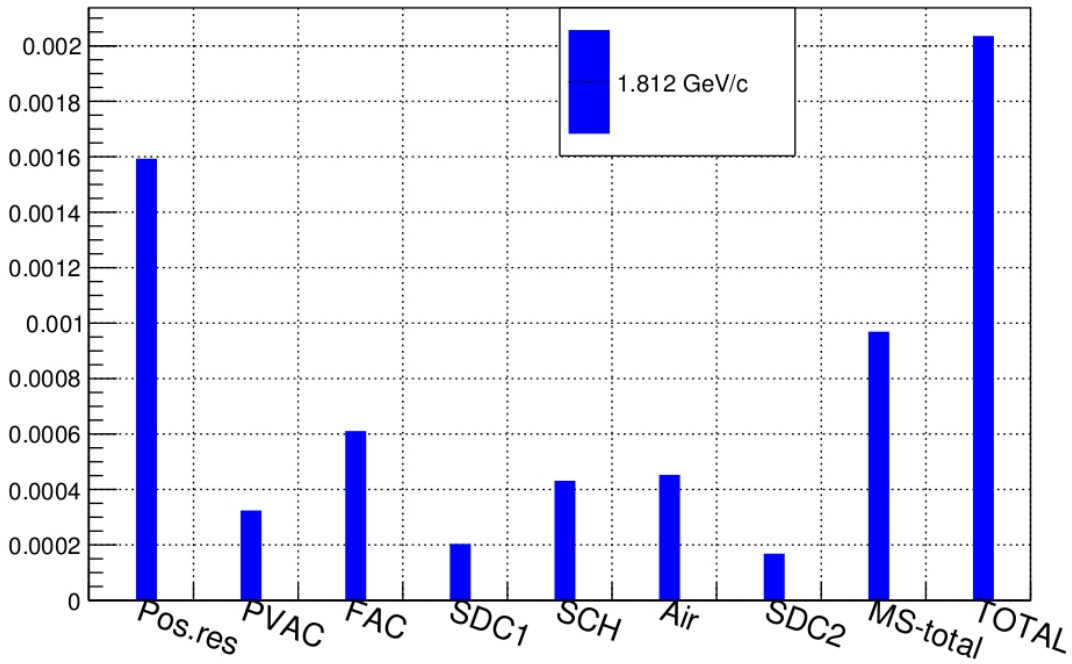

Figure 4.4: The angle resolution of K^- in the KURAMA spectrometer setup.

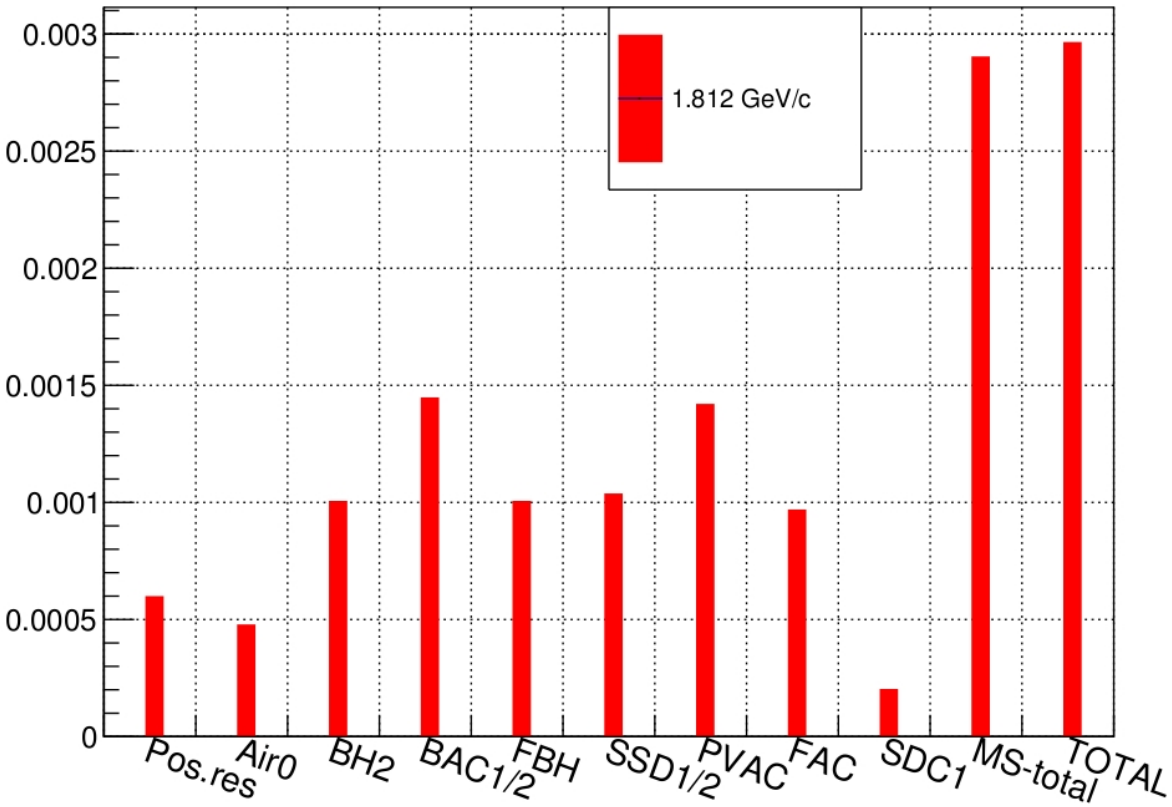

Figure 4.5: The angle resolution of each device before and after the target position of the E07 experiment.In the vicinity of figure for the total MS's, major contributions are belong to mainly BAC1/2 and PVAC Aerogel counters.

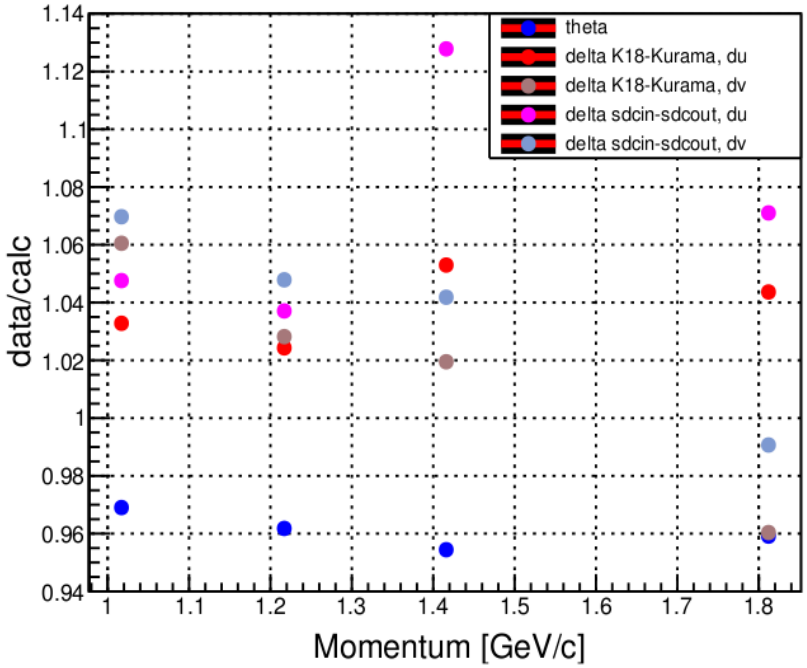

Figure 4.6: Comparison of data and calculation of: bending angle and small scattering angles.

The missing mass resolution

The missing mass resolution is determined from the next mathematical equation, so

$$\Delta M^2 = (\frac{\delta M}{\delta p_{K-}})^2 \delta p_{K-}^2 + (\frac{\delta M}{\delta p_{K+}})^2 \delta p_{K+}^2 + (\frac{\delta M}{\delta \theta})^2 \delta \theta^2$$

As we can see from the equation, MM resolution contributions are comes from the next: incident beam momenta, scattered particle's momenta and angle. However, at first the incident beam contributions are ignored due to the good momentum resolutions of it. In that case, only contributions of the scattered particle's momentum and angle are calculated. In this section we discuss about missing mass resolution calculation. And each contribution of MM are described in details and calculation of MM resolution will be provided to make comparison with the data analysis.

Therefore, we continue only with 2 parts, scattered and angle resolutions.

$$\frac{\delta M}{\delta p_{K+}} = -\frac{1}{M}[\beta_{K+} \cdot (M_{tgt} + E_{K-}) - p_{K-} \cos\theta] \tag{4.11}$$

$$\frac{\delta M}{\delta \theta} = -\frac{p_{K-}p_{K+}}{M}(\sin\theta) \tag{4.12}$$

where δp_{K-} and δp_{K+} are the momentum resolutions of incoming and outgoing particles, accordingly. $\delta\theta$ - the angluar resolution of the reactin angle. For estimating the missing mass resolution of the (K^-, K^+) reaction in polyethylene target, formulae of the kinematics of missing mass is crucial. At the beginning,we should evaluate the missing mass contributions, such from the scattered and angular parts of the total.

Here, we introduce the deriviation of missing mass partions respect to outgoing momenta, actually scattered $K+$. The equations (4.12) and (4.13) can be derived from (3.5).

$$M_x = \sqrt{(E_{K-} + M_{tgt} - E_{K+})^2 - (p_{K-}^2 + p_{K+}^2 - 2p_{K-}p_{K+}cos(\theta_{K^-K^+})}$$

$$\frac{\delta M}{\delta p_{K+}} = \frac{\delta((E_{K-} + m_{tgt} - E_{K+})^2 - (p_{K-}^2 + p_{K+}^2 - 2p_{K-}p_{K+}cos\theta))^{1/2}}{\delta p_{K+}} =$$

$$= \frac{1}{2M}[2(E_{K-} + m_{tgt} - E_{K+})(-\frac{\delta E_{K+}}{\delta p_{K+}}) - (2p_{K+} - 2p_{K-}cos\theta)]$$

where we determine $\frac{\delta E_{K+}}{\delta p_{K+}}$ as follows,$E^2 = p^2 + m^2$(relativistic form of kinematics)

$$\frac{\delta E_{K+}}{\delta p_{K+}} = \frac{\delta\sqrt{p_{K+}^2 + m_{K+}^2}}{\delta p_{K+}} = \frac{1}{2}(p_{K+}^2 + m_{K+}^2)^{-1/2} \cdot 2p_{K+} = \frac{p_{K+}}{E_{K+}}$$

after substitution and taking into account the next $\beta = \frac{p}{E}$

$$-\frac{1}{M}(E_{K-} \cdot \frac{p_{K+}}{E_{K+}} + m_t \cdot \frac{p_{K+}}{E_{K+}} + E_{K+} \cdot \frac{p_{K+}}{E_{K+}} - p_{K+} - p_{K-}cos\theta)$$

$$= -\frac{1}{M}(\beta_{K+}(E_{K-} + m_t) - p_{K-}cos\theta)$$

Finally, we proved the derivative of MM contribution in case of outgoing $K+$. In addition,the reaction angle parts:

$$\frac{\delta M}{\delta \theta} = \frac{\delta((E_{K-} + m_{tgt} - E_{K+})^2 - (p_{K-}^2 + p_{K+}^2 - 2p_{K-}p_{K+}cos\theta))^{1/2}}{\delta\theta} =$$

$$\frac{1}{2M}[(2p_{K-}p_{K+}cos\theta)]$$

derivation of cos gives -sin, so final, so

$$\frac{\delta M}{\delta \theta} = -\frac{1}{M}[(p_{K-}p_{K+}sin\theta)].$$

The next parameters are taken to count the missing mass resolution

- M_{tgt} – target mass (proton mass, 938.3 MeV/c2)
- β_{K+} 0.935 (in the 1.3 GeV/c momenta)
- E_{K-} 1.865 Gev (energy of incident beam)
- M – expected particle mass (Ξ^- , 1.327 GeV/c2 [PDG table])
- p_{K-} 1.8 GeV/c, incident beam momenta
- p_{K+} 1.3 GeV/c, typical momentum of the scattered particle
- $\Delta\theta$- angle 0.0026955 [rad]. Scattering angle resolution of K^+.
- $\Delta p(kaon) = 0.0182$ (sigma) [1.3 GeV/c beam].Mom.res of scattered K^+.
- $\theta = 0.1923$ rad [11 degree], scattering angle of $K+$

After calculation, scattered particles contribution:

$$\frac{\Delta M}{\Delta p_{K+}} = -0.837$$

while, angle contribution is:

$$\frac{\Delta M}{\Delta \theta} = -0.95931$$

The contributions: $\Delta M_{K+} = 0.000232\ GeV/c^2$ and $\Delta M_\theta = 8.06E-006\ GeV/c^2$. According to the examined contributions, it is easy to notice that the momentum resolution plays main role in a state estimating missing mass resolution. In other words, the partion of angle resolutions is minor compare to the momentum resolution.The calculated missing mass resolution was around:

$$\Delta M_{calc} = 15.23 MeV/c^2$$

for the $p(K^-, K^+)\Xi^-$ reaction. Analysis result was

$$\Delta M_{data} = 15.76 MeV/c^2,$$

The ratio of:

$$\frac{\Delta M_{data}}{\Delta M_{calc}} \approx 1.03$$

We can see that the ratio of data and calculation was ~ 1.03. To conclude that the obtained missing mass magnitudes are in good agreement.

Chapter 5

Conclusion

The E07 experiment was performed at the K1.8 beam line in the J-PARC Hadron experimental facility. The goal of E07 experiment is a study of of double Λ hypernuclei generating Ξ^- particle's systems using hybrid-emulsion on the diamond target. In the experiment 1.8 GeV/c K^- beam was used as an incident beam and the scattered particle K^+ had been detected by the KURAMA spectrometer system from $p(K^-, K^+)\Xi^-$ reaction.

Here, we have showed the momentum and angle resolutions of incident particle using KURAMA magnet system. Namely, the performance of the KURAMA spectrometer is verified by investigating momentum and angle analysis with 4 data sets of different beam momenta values(beamthrough run): 1.0,1.2,1.4 and 1.8 GeV/c,respectively. Missing mass resolution analysis of $p(K^-, K^+)\Xi^-$ reaction based on momentum and angular resolution of the spectrometer. For the missing mass analysis we used CH_2 target run. The Ξ^- particle is generated by the irradiation of K^- beam on the polyethylene target.

Finally, the comparison of calculation and analysis result were made for momentum, angle and missing mass resolutions. And comparison displays, that the ratio of data and calculation was for momentum resolution $\sim 0.83 - 1.05$ and $\sim 0.96 - 1.13$ for angle resolution. According to figures 4.1 and 4.6, calculation and analysis results are consistent for momentum and angle resolutions. For the missing mass resolution, the ratio of data and calculation was ~ 1.03 at the final stages. It means, for the missing mass analysis, the values for data and calculation are in good agreement.

To conclude, that the performance of KURAMA spectrometer system is probed by the effect of position resolution of tracking detectors and multiple scattering by each experimental devices which are in the E07 experiment. Therefore, the KURAMA spectrometer system works well as we expected in the E07 experiment.

Bibliography

[1] B.Povh et al., *Particles and Nuclei*, Graduate Texts in Physics, (2015)

[2] Martin B.R., *Nuclear and Particle Physics*, (2009)

[3] K.Nakazawa et al. J-PARC proposal E07, Title: "Systematic study of Double Strangeness System with an Emulsion – Counter Hybrid method", 2016

[4] Horsley, R. et al. Octet baryon mass splittings from up-down quark mass differences. PoS LATTICE2012 (2012) 135 arXiv:1212.5507

[5] V.L. Highland, Nucl. Instrum. Methods 129 , 497 (1975); Nucl. Instrum. Methods 161,171 (1979).

[6] G.R. Lynch and O.I Dahl, Nucl. Instrum. Methods B58, 6 (1991).

[7] M. Danysz, et al., Nucl. Phys. 49 (1963) 121

[8] R.H.Dalitz et .al., Proc. R. Soc. Lond. A426 (1989)

[9] K.Shirotori. Master Thesis. Tokohu University (2006)

[10] I.Ichikawa. Master Thesis. Osaka University (2015) [in Japanese]

[11] R. Honda. Study of ΣN interaction in nuclei using meson beams, Doctor Thesis (2014)

[12] K. NAKAZAWA. Double-Λ Hypernuclei via the Ξ^- Hyperon Capture at Rest Reaction in a Hybrid Emulsion. Nuclear Physics A 835 (2010) 207–214

[13] William R.Leo. *Techniques for Nuclear and Particle Physics Experiments*. (1994)

[14] Particle Data Group (PDG), htpp://www.pdg.lbl.gov

Chapter 6

Acknowledgements

I would like to thank Dr. Tadafumi Kishimoto for the guidance and support he provided me during my studies. He is also responsible for me being at Osaka University and undertaking this study. I am very grateful for the opportunity he gave me.

I would like to thank heartfully to Professor Atsushi Sakaguchi, who helped me during my study at Osaka University. Since joining the Hyper group, he put a lot of effort to understand the experiment features and analyze it correctly. Also I appreciate his contribution deeply, because he spent lots of time to write correctly my master thesis. Not only master thesis, but also he gave me valuable advice and suggestions about physics experiment. He is one of the best person to talk about everything.

I would like to thank Professor Noumi who is one of the referees in my master's defense of degree.

I would like to thank Emi Matsuda-san who helped me a lot in a state of daily life in Japan. She is one of the best person who I met in Japan.

I also would like to special thanks Hyper group members, namely Ph.D students Shuhei Hayakawa and Minami Nakagawa. They are helped me a lot in a case of analysing experimental data. I wish them a luck of life in their future.

I would like to thanks for Kishimoto lab members and I wish them success and would receive their master-doctorate degrees as they dreamed.

I also special thanks to my family members and relatives who have supported me to finish my study in Japan.